APPLICATION OF COMPRESSIVE SENSING FOR EFFICIENT SPECTRUM SENSING AND DETECTION USING COGNITIVE RADIO

BY

NADIA IQBAL

Thesis submitted to the faculty of Electrical Engineering, Military College of Signals, National University of Sciences and Technology, Pakistan, in partial fulfillment for the requirements of MS degree in Electrical Engineering

March 2014

ABSTRACT

Compressive Sensing (CS) is a novel signal processing paradigm which has found great interest in many applications including communication theory and wireless communications. In wireless communication, CS is particularly suitable for its application in the area of spectrum sensing for cognitive radios, where the complete spectrum under observation, with many spectral holes, can be modeled as a sparse wide-band signal in frequency domain.

In this work, the CS framework is extended for the estimation of wide-band spectrum by reconstructing the spectrum using compressive sensing matrix and reduced time samples of the wide-band signal. The proposed algorithm outperforms conventional channel-by-channel scanning in a sense that sensing time is reduced. The Mean Square Error (MSE) estimation of the reconstructed spectrum via MATLAB simulations shows that a better approximation of the reconstructed spectrum is obtained even when the number of time samples is reduced, such that the vacant channels can be identified. The wide-band signal detection is also performed via CS using cognitive Bayesian energy detector, which shows that as the number of wide-band filters is increased, probability of detection of CS algorithm improves. Bayesian Compressive Sensing (BCS) framework is also modified for the recovery of a sparse signal, whose non-zero coefficients follow a Rayleigh distribution. It is then demonstrated via simulations that MSE significantly improves, when appropriate prior distribution is used for the faded signal coefficients. Different parameters for the system model, e.g., sparsity level, number of measurements, etc., are then varied to show the consistency of the results for different cases.

Dedicated to my Father

Sqn. Ldr. Muhammad Iqbal Saqib

(Retd.)

ACKNOWLEDGMENTS

First of all I would like to humbly thank ALLAH Almighty, the most gracious and the most merciful for giving me the opportunity, strength, courage and good health to complete my thesis in due time.

I would like to express my deepest gratitude to my honorific supervisor Dr Abdul Ghafoor for his continuous help, advice and guidance in fulfilling this task.

I am very much obliged to Dr Asad Mahmood for his useful suggestions and advice that helped me a lot in completion of my thesis. He helped me a lot in having a deep insight into the topic.

I specially want to thank my advisor Dr Sajjad Hussain for his constant source of guidance, encouragement and advice. He always responded to my questions and queries so promptly. I am really very grateful to him.

I also want to thank Dr Abdul Rauf, Dr Adil Masood and Dr Imran Rasheed for being my committee.

Last but not the least; I place my sense of gratitude to my parents and my family, who have always been source of inspiration for me. It is all due to their tenderness and devotion, that I have been successful in every field of my life. My sister Dr. Sadia Iqbal has always motivated me and built up my confidence. Special thanks to my friends Hina Khan and Saadia Tabassum who encouraged me and supported me throughout my degree.

LIST OF ACRONYMS

Acronym	Meaning
FCC	Federal Communications Commission
CR	Cognitive Radio
WLAN	Wireless Local Area Networks
SNR	Signal-to-Noise Ratio
CS	Compressive Sensing
BCS	Bayesian Compressive Sensing
DSA	Dynamic Spectrum Access
BP	Belief Propagation
AWGN	Additive White Gaussian Noise
PDF	Probability Density Function
RF	Radio Frequency
DSP	Digital Signal Processing
MAP	Maximum A-Posterior
SIR	Signal-to-Interference Ratio
xG	NeXt Generation
ML	Maximum Likelihood
MSE	Mean Square Error

Contents

INTRODUCTION **1**

1.1 Overview **1**

1.2 Problem Statement **2**

1.3 Proposed Solution **3**

1.4 Objectives **4**

1.5 Contribution **4**

1.6 Organization of Thesis **6**

1.7 Summary **7**

LITERATURE REVIEW **8**

2.1 Introduction **8**

2.2 Cognitive Radio (CR) **8**

2.2.1 Cognition Cycle of a CR 8

2.2.2 Applications of CR 10

2.2.2.1 Dynamic Spectrum Access (DSA) 10

2.2.2.2 Military Applications 11

2.2.2.3 Public Safety 11

2.2.2.4 Broader and Commercial Application 12

2.2.2.5 CRs and MIMO 12

2.2.2.6 CR Technology in xG Networks 12

2.3 Spectrum Sensing using CR **14**

2.3.1 Matched Filtering 16

2.3.2 Energy Detection 17

2.3.3 Cyclo-stationary Feature Detection 19

2.4 Co-operative Spectrum Sensing 20

2.4.1 Centralized Sensing 21

2.4.2 Distributed Sensing 21

2.5 Wide-band Spectrum Sensing using CR 21

2.5.1 Compressive Sensing (CS) Theory 23

2.5.2 Bayesian Compressive Sensing (BCS) 27

2.5.3 Prior Models for Belief Propagation 30

2.5.3.1 Two State Gaussian Mixture 30

2.5.3.2 Gaussian-Spike Prior Model 31

2.5.3.3 Rayleigh-Spike Prior Model 32

2.6 Summary 33

COMPRESSIVE SENSING AND DETECTION OF WIDEBAND SPECTRUM USING CR 34

3.1 Introduction 34

3.2 Problem Statement 34

3.3 Wideband Spectrum Reconstruction via CS with Reduced Delay and Complexity 35

3.4 Wideband Signal Detection via CS Using Cognitive Bayesian Energy Detector 38

3.5 Summary 41

CS FRAMEWORK FOR RAYLEIGH FADING CHANNELS USING BAYESIAN INFERENCE APPROACH 42

4.1 Introduction 42

4.2 Problem Formulation 43

4.3 Proposed System Model 45

4.3.1 Sparse Sensing Matrix 46

4.3.2 Prior Model 46

4.3.2.1 Prior Model for Noiseless System Model 47

4.3.3.2 Prior Model for Noisy System Model 48

4.4 CS Decoding via BP 49

4.5 Advantages over previous algorithms 55

4.6 Summary....55

SIMULATIONS AND REULTS 56

5.1 Introduction....56

5.2 Wide-Band Spectrum Reconstruction via CS with Reduced Delay and Complexity....56

5.2 Detection of Wide-band Signal via CS using CR Bayesian Energy Detector....65

5.3 Bayesian Compressive Sensing Framework for Rayleigh Fading Channels....67

CONCLUSION AND FUTURE PERSPECTIVE 75

6.1 Conclusion 75

6.2 Future Perspective 76

BIBLIOGRAPHY....77

List of figures

Figure: 2.1: Cognition cycle of CR 9

Figure: 2.2: Applications of a CR 10

Figure: 2.3: Functions of CR in xG networks 13

Figure: 2.4: Probabilities of detection and missed detection 15

Figure: 2.5: Probability of false alarm 15

Figure: 2.6: Matched filter based spectrum sensing 17

Figure: 2.7: Energy detection based spectrum sensing 18

Figure: 2.8: Cyclo-stationary based spectrum sensing 19

Figure: 2.9: Nyquist sampling 24

Figure: 2.10: Compressive sampling 26

Figure: 2.11: Factor graph illustration 28

Figure: 3.1: Compressive sampling by inserting columns of zeros in sensing matrix 37

Figure: 3.2: Compressive sampling by distributing columns of zeros in sensing matrix.....37

Figure: 4.1: Message passing between signal nodes and measurement nodes 53

Figure: 5. 1: Wide-band spectrum, 5 out of 10 active channels, SNR = 10 dB.....58

Figure: 5. 2: Reconstructed spectrum, M = N/2, S = N/2 59

Figure: 5. 3: Reconstructed spectrum, M = N/2, S = N/4 59

Figure: 5. 4: Reconstructed spectrum, M = N/2, sub-Nyquist sampling rate = 2/3 60

Figure: 5. 5: MSE estimated for reconstructed spectrum using different number of linear combinations and time samples 62

Figure: 5. 6: MSE estimated for reconstructed spectrum at sub-Nyquist sampling rates.....63

Figure: 5. 7: MSE performance of CS algorithm for wide-band spectrum reconstruction when number of active channels are varied to vary the sparsity level of the spectrum (M = N/2, S = N/2) 64

Figure: 5. 8: MSE performance of CS algorithm for wide-band spectrum reconstruction when number of active channels are varied to vary the sparsity level of the spectrum (M = N/2, sampling rate = 2/3 of Nyquist rate) 65

Figure: 5. 9: Probability of detection curve for detection of wide-band signal via CS.....66

Figure: 5. 10: Probability of false alarm curve for detection of wide-band signal via CS 67

Figure: 5. 11: MSE as a function of M using different matrix row weights R for BCS recovery of Rayleigh faded signal using prior composed of convolution of Rayleigh-Gaussian distribution and Spike distribution, (N = 1000, K = 20, M = N/2) 69

Figure: 5. 12: MSE as a function of sparsity level K for BCS recovery of sparse Rayleigh faded signal using prior composed of convolution of Rayleigh- Gaussian distribution and Spike distribution, (N = 200, 500, 1000, M = N/2) 70

Figure: 5. 13: MSE as a function of number of measurements M using different number of samples for prior distribution p for BCS recovery of Rayleigh faded signal using prior composed of convolution of Rayleigh-Gaussian distribution and Spike distribution, (N =1000, K= 20, M = N/2) 71

Figure: 5. 14: MSE as a function of noise variance where BCS recovery of sparse Rayleigh faded signal is done for noisy model using two types of priors, i.e., (1) Prior composed of convolution of Rayleigh-Gaussian distribution and Spike distribution (Rayleigh- Gaussian-Spike) (2) Gaussian-Spike prior (Gaussian-Spike) (N = 1000, K = 20, M = N/2) 72

Figure: 5. 15: MSE as a function of number of measurements M where BCS recovery of sparse Rayleigh faded signal is done for noisy model using two types of priors, i.e., (1) Prior composed of convolution of Rayleigh-Gaussian distribution and Spike distribution (N = 500, K = 20, R = 20).....73

Figure: 5. 16: MSE as a function of sparsity level K where BCS recovery of sparse Rayleigh faded signal is done for noisy model using two types of priors, i.e., (1) Prior composed of convolution of Rayleigh-Gaussian distribution and Spike distribution, (2) Gaussian- Spike prior (N = 500, M = N/2, noise variance = 1).....74

Chapter 1

INTRODUCTION

1.1 Overview

Rapid growth and development in mobile communications, satellite communications and other wireless communication systems require advanced spectrum sources. Within the current spectrum framework, different spectrum bands are allocated to specific licensed users. The licensed users of the spectrum are known as the primary users, who possess the legacy right to use the frequency bands allocated to them. The licensing process of the spectrum and allocating fixed ranges of spectrum bands to the licensed users results in congestion in those bands, while lot of spectrum bands are under-utilized and apparently causes spectrum scarcity [1]. The spaces in the spectrum bands which are not being actively used by the licensed users are called spectral holes. To efficiently utilize the spaces in the spectrum and solve the problem of under-utilization of spectrum, Federal Communications Commission (FCC) has allowed unlicensed/secondary users to sense the spectral holes and utilize them using Cognitive Radio (CR) technology [2-4]. Spectrum utilization can be made efficient, when secondary users sense the spectrum and detect the spectral holes accurately and utilize them efficiently without causing any interference to the transmission of other users. Thus, secondary users must possess cognitive capabilities to sense the spectrum reliably and detect the spectral holes in it.

The emerging paradigm of Dynamic Spectrum Access (DSA) [5] makes sure that the spectrum scarcity problem is solved by allowing secondary/unlicensed users to utilize the already allocated spectrum dynamically using spectrum agile wireless networks [6]. The

key component to DSA paradigm is CR which senses its environment and performs such functions to serve its users, without causing any harmful interference to the neighboring authorized users [7]. With the use of CR, secondary users coexist with the licensed users without causing any interference in their transmission to increase the efficiency of the spectrum. Thus CR provides an opportunistic sharing of the spectrum. Dynamic allocation of the spectrum via CR has made advancement in signal processing capabilities and wireless technology. To sense the spectrum in minimum possible time at low signal-to-noise ratio (SNR) is one of the critical issues faced by CR in spectrum sensing.

1.2 Problem Statement

In mobile communications, satellite communications and other wireless communication systems, when radio waves transmit from the transmitter, they undergo scattering, reflection and diffraction, thus creating multi-path effect. In consequence, the received signal level undergoes fluctuations and changes in amplitudes and phases of the signal occur. This phenomenon is called fading and due to such phenomena, more study of practical channels like Rayleigh fading channels, is needed along with that of classical Additive White Gaussian Noise (AWGN) channel. The Rayleigh fading channels should be considered while sensing and detection of such wide-band signals. A CR promises the sensing and detection of such wide-band signals in Rayleigh fading channels. However the traditional approach to sense the wide-band spectrum and search for the available bandwidth for secondary usage is channel-by-channel sensing techniques like energy detector based sensing [8], waveform based sensing [9], cyclo-stationary based sensing [10]. This channel-by-channel scanning of wide-band spectrum becomes costly and complex because it requires a Radio Frequency (RF) front end with numerous tunable

and narrow band-pass filters. Such methods also introduce latency in the sensing of the wide-band spectrum. Since the secondary users are allowed to sense the spectrum within least/ minimum time possible such that there is no interference caused in the transmission of the primary users. Channel-by-channel scan will render more time in sensing; causing interference to the transmission of primary users, when they become active.

1.3 Proposed Solution

To facilitate wide-band spectrum sensing, Compressive Sensing (CS) [11-12], has emerged as a fascinating method of acquisition of wide-band signals at rates that are significantly lower than Nyquist rates. Faster methods are being explored to sense the spectrum because the occupancy of a frequency band changes rapidly. CS minimizes the sampling time by using a smaller number of linear combinations out of the signal. The information contained in the few large coefficients can be encoded by few random linear projections, while throwing away rest of the coefficients that might be useless in further signal processing application. Those encoded random projections can then be used to decode the signal [13].

The under-utilization of the spectrum creates spectral holes in the assigned frequency bands; thus such signals are created that are sparse in nature. CS is such a sampling method that samples fewer measurements from the sparse signal. The sparsity feature in the wide-band signals motivates to sense such signals compressively, such that the frequency representation of sparse signals is reconstructed using lesser number of time samples compared to those imposed by Nyquist theorem. When CS is used to sense the wide-band spectrum using CR, the whole spectrum is sensed at once; thus delay and complexity created by channel-by-channel scan can be avoided using CS technique [14].

The CS method can be further simplified using Bayesian inference, provided the system model supports Bayesian approach. Since the Bayesian inference provides solutions that are conditional on the observed data, it estimates a full probability model, where probability distributions are associated with parameters or hypotheses and decoding the signal is considered as Maximum A-Posterior (MAP) estimation problem. Bayesian Compressive Sensing (BCS) accomplished with Bayesian inference provides precise estimation of signal and reduces the number of measurements for CS decoding [15-16].

1.4 Objectives

The main objective is to propose a solution to high data rates requirement in wide-band spectrum sensing. Latency caused due to traditional scanning techniques can cause interference to primary transmission. Reducing the delay via CS approach can make the wide-band spectrum sensing more efficient. Also the inherent feature of fading in wireless communication is usually not considered in sensing techniques. The performance of the sensing algorithms varies for faded signals. CS algorithm using Bayesian inference approach is proposed for the signal propagation in Raleigh fading channels.

1.5 Contribution

The CS algorithm has been modified to estimate the wide-band spectrum such that the delay as well as complexity in wide-band spectrum sensing is reduced. Also the usage of BCS framework for spectrum sensing has been explored in a practical wireless channel like Rayleigh fading channel.

In first approach, CS algorithm is used for estimation of wide-band spectrum to identify the vacant channels in the reconstructed spectrum in reduced time. In this approach,

lesser number of time samples is taken out of the signal, instead of taking all the samples of the signal, and the wide-band spectrum is reconstructed using a compressive sensing matrix. The CS matrix reconstructs a better approximation of the wide-band spectrum even with reduced number of linear combinations, such that the occupied channels in the spectrum can be identified. The wide-band spectrum estimation is performed with reduced delay.

In second approach, the sensing matrix used in CS algorithm is simplified by introducing columns of zeros in it such that compressive sampling is performed at sub-Nyquist rate. In this case also, a good approximation of reconstructed wide-band spectrum is obtained to identify the vacant bands in it.

To further investigate the performance of the sensing algorithms in practical channels, BCS algorithm has been modified according to the signal propagation in Rayleigh faded channels. The performance of different algorithms will vary for signal propagation in a free space model or AWGN channel and for signal propagation in Rayleigh fading channel. The signal undergoes fading in a Rayleigh fading channel due to the multi-path effect, and the performance of the signal processing /detection algorithms will be affected due to the fading phenomenon. To overcome this problem, the BCS framework has been modified according to the Rayleigh fading channels such that appropriate priors are chosen for the decoding of the Rayleigh faded signal via Belief Propagation (BP). Our results show that when an appropriate prior is used according to the system model, the recovery of the signal improves which has been demonstrated via an improvement in Mean Square Error (MSE). We demonstrated that varying different parameters like sparsity level, number of measurements etc., has an impact on the MSE performance of

the algorithm. When prior is chosen wisely according to the system model, then MSE can be further reduced by varying these parameters.

1.6 Organization of Thesis

This document is divided into six chapters.

Chapter 1 begins with the introduction/overview, problem statement, proposed solution, objectives and contribution. An overview of the proposed algorithm is also given in this chapter.

Chapter 2 provides the literature review, brief description of conventional methods for spectrum sensing, problems faced during wide-band spectrum sensing and an overview of CS and CS via BP algorithm. Application of CS for efficient wide-band spectrum sensing has also been discussed.

Chapter 3 provides the complete overview of the proposed CS algorithm for reconstruction of wide-band spectrum using ℓ_1-minimization, to identify the occupied bands in the spectrum. The detection of wide-band signal using a compressive Bayesian energy detector has also been discussed.

Chapter 4 covers the Bayesian inference approach for wide-band signal detection using CS. BP algorithm to estimate the MAP probability of signal elements, is modified according to the signal propagation in Rayleigh fading channels.

Chapter 5 presents the simulation results of the proposed CS and BCS algorithms in different scenarios. MSE estimation suggests improvement in the sensing algorithms by varying different parameters.

Chapter 6 concludes this thesis document. It also highlights the future research directions.

1.7 Summary

This chapter covers the background and concepts of wide-band spectrum sensing, CR, CS, CS via BP. It also covers the overview, problem statement, objectives and the proposed technique.

Chapter 2

LITERATURE REVIEW

2.1 Introduction

In this chapter, some important concepts related to spectrum sensing using CR are discussed. We review some conventional techniques, proposed in literature to sense the spectrum using CR. Some insight into the wide-band spectrum sensing techniques has also been made. The concepts of CS and BCS and their application in wide-band spectrum sensing have also been demonstrated in this chapter.

2.2 Cognitive Radio (CR)

A CR is a software defined radio that can change its transceiver parameters based on its interaction with the environment in which it operates [7]. A CR incorporates multiple sources of information, determines its current operating settings, and collaborates with other CRs in a wireless network [2-4]. It efficiently utilizes the wide-band spectrum in an intelligent and effective way by coordinating with other CRs in the network regarding the usage of spectrum to identify the unused radio spectrum on the basis of its observation. This unused spectrum might be owned by some licensed primary user. The CRs make spectrum utilization efficient by sharing spectrum for secondary transmission. To prevent interference caused in the primary transmission, CRs provide cognition in spectrum utilization along with cognition in its numerous applications [4-5].

2.2.1 Cognition Cycle of a CR

The cognition cycle of a CR is “top level control loop for CR” as shown in Figure 2.1 [4].

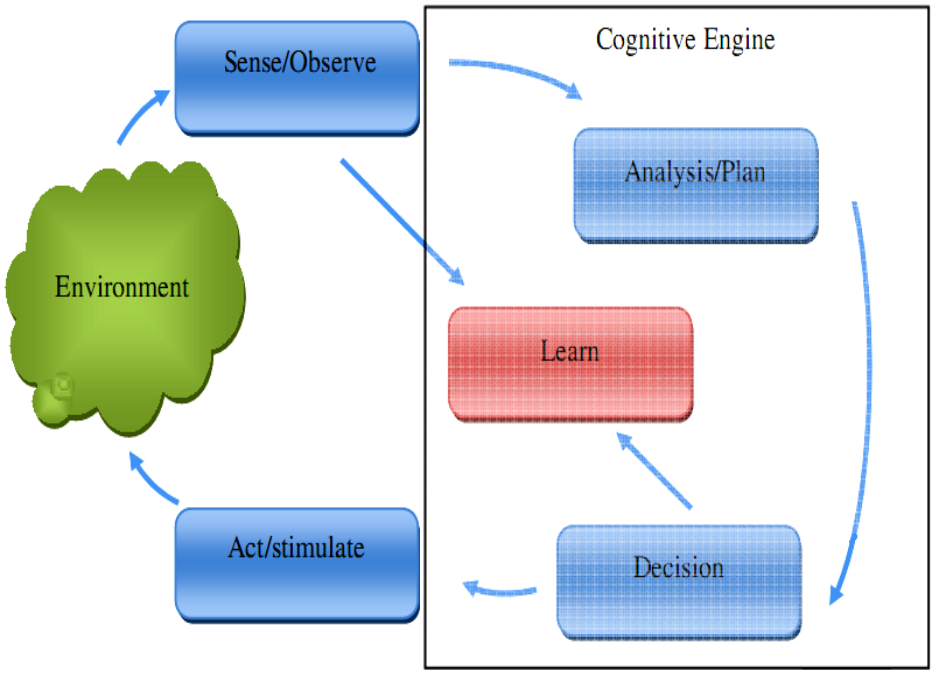

Figure: 2.1: Cognition cycle of CR

In cognition cycle, the CR receives information by directly observing (Sense/Observe) its surrounding environment. The information obtained is then analyzed (Analysis) to determine the effectiveness of the information. The CR, then, determines its alternatives (Plan) based on that evaluation. And then it chooses the alternative (Decision) that would improve its valuation. The CR then implements its plan (Act) by adjusting its various parameters and other sources and performs according to the adjusted resources (Stimulate). The environment is continuously observed by the CR to avoid any possibility of interference. It utilizes all its observations and planning according to the changes in the environment to improve its performance (Learn) continuously [3].

2.2.2 Applications of CR

A CR promises to improve the utilization of spectrum resources through reduced engineering and planning time, and adaptation to current operating conditions. It finds its applications in various areas as shown in Figure 2.2 [17]:

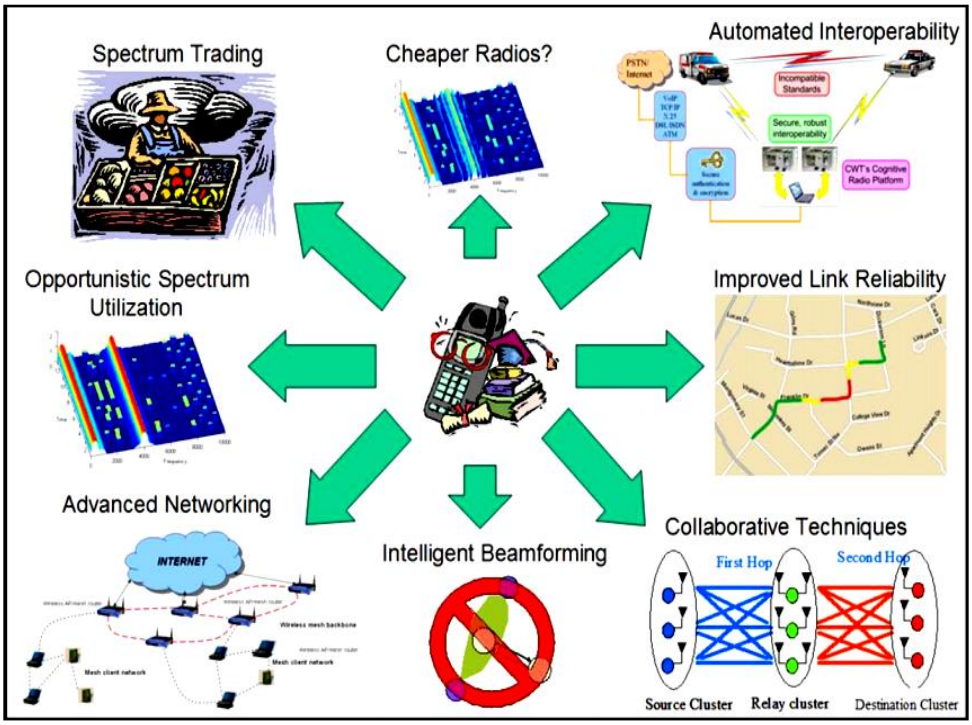

Figure: 2.2: Applications of a CR

2.2.2.1 Dynamic Spectrum Access (DSA)

DSA is considered as the prime candidate in terms of practical application of a CR technology [18]. DSA is real-time adjustment of utilization of the spectrum according to the changes in the circumstances and the environment. Generally, DSA implies that the licensed spectrum is made available for the secondary usage, when the primary user is not active. Secondary spectrum sharing is possible until and unless there is no significant interference caused to the primary transmission. Recently in 2008, the FCC allowed the

secondary usage of TV-band spectrum via CR with a condition of minimal impact on the original TV signals and wireless microphone signals being broadcasted [19].

2.2.2.2 Military Applications

The military community has recognized the benefits of using CR technology in enhancing military/tactical capabilities, particularly in distributed communications, integration of joint forces, intelligence and surveillance systems [20]. With frequency agility and/or flexibility in the radio systems, the interoperability between them can be enhanced. Also the detection of interferers to the communication system via CR technology has made it a must-have technology for military applications. CR technology offers advantages in defense applications in terms of protecting the communication transmissions and recognizing the enemy communications [21].

2.2.2.3 Public Safety

Public safety system is another area in which CR technology can offer great advantages [22]. Current public safety systems have limited capabilities, since these are configured and predefined into the radio based on the roles and responsibilities assigned to the radio user. CR technology offers reprogramming the radio systems with different channel/frequency assignments and functions. To enhance frequency utilization and interoperability in public safety communication systems, CRs enable such devices as to bridge the communication between safety systems that are operating at different frequencies. To maintain the call priority and improve the response time for emergency systems, CRs effectively utilize the existing spectrum [23].

2.2.2.4 Broader and Commercial Application

As the wireless technologies and Wireless Local Area Networks (WLAN) like 802.11 are proliferating in the ISM band, interference to the neighborhood transmission is becoming problematic. This results in the degradation of the performance of the technology. Different technologies are currently utilizing some adaptive techniques to identify channels, select dynamic frequency and modulation, to obtain higher data throughput, they are still required to follow the standards that limit their performance [24]. By using the CR in the RF environment like the Industrial, Scientific And Medical (ISM) radio band, it provides a platform for us to enhance the performance of the current systems especially in terms of interference being caused [25].

2.2.2.5 CRs and MIMO

Multiple Input Multiple Output (MIMO) smart antenna systems are used in communications for improved performance (such as enhanced data rate or link reliability) and added capability (such as beam forming) [26]. The CR is being used with MIMO to adapt the employed MIMO scheme to the needs of the environment and user during use to create a more effective relaying scheme. These led to reported improvements in link capacity, link reliability, range, network availability and energy usage [27].

2.2.2.6 CR Technology in xG Networks

NeXt Generation (xG) communication networks, also known as DSA networks as well as CR networks provide higher data rates to the mobile users by adopting DSA techniques [28].

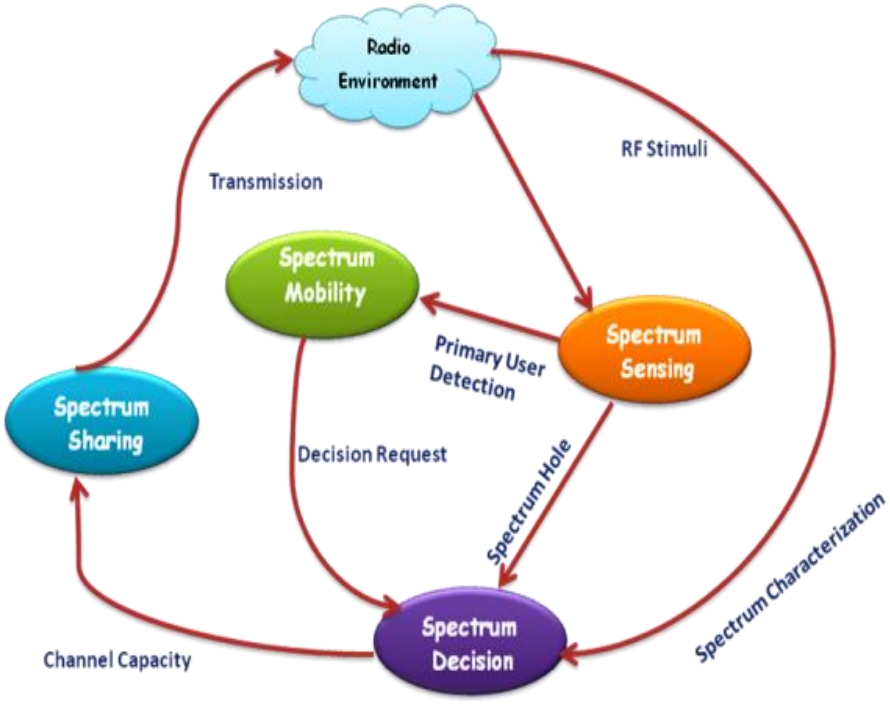

Figure: 2.3: Functions of CR in xG networks

The underutilization of the existing spectrum can be made efficient by allowing secondary users to access the spectrum opportunistically without interfering with the primary users in the xG networks [29].

The main functions of CR in xG networks can be summarized as shown in Figure 2.3 [5]:

• **Spectrum sensing:** To detect the vacant channels in the spectrum and share the spectrum without causing any harmful interference to other users.

• **Spectrum management:** To manage the spectrum utilization according to the user communication requirements.

• **Spectrum mobility:** To maintain the seamless communication while transiting to other frequency band.

• **Spectrum sharing:** To provide fair usage of the spectrum by scheduling methods with other xG users.

2.3 Spectrum Sensing using CR

The main challenge that a CR faces while sensing the spectrum is to detect the signal in least possible time and make a correct decision about the availability of the vacant space in the spectrum.

In general, the binary hypothesis testing theory [30] can be well applied to evelaute the performance and capability of any CR system used for spectrum sensing. The two hypothesis i.e., H_0 or $Hypothesis\ 0$ and H_1 or $Hypothesis\ 1$ form the basis of binary hypothesis testing. In the context of CR, the absence of the primary user can be represented by H_0, where as the presense of primary user can be represented by H_1. The performance of a CR system is evaluated on the basis of its probability of making an accurate or false decision. If γ is defined as the threshold value for each hypothesis, the Probability Density Function (PDF) under each hypothesis can be shown in Figure 2.4 and Figure 2.5.

The probability that CR declares the primary signal, at hypothesis H_1, when the primary user is active is known as probability of detection i.e., P_d. In this case, the PDF is higher than the threshold γ as shown in Figure 2.4. Similarly the probability that a CR misses the primary signal, when the primary user is active is known as probability of missed detection i.e., P_m which is the PDF value lesser than the threshold γ.

When a CR declares the presence of primary signal, when the primary user is not active in actual, the probability of making false decision is known as probability of false alarm i.e., P_{fa}. In this case the PDF under hypothesis H_0 is higher than threshold γ as shown in Figure 2.5.

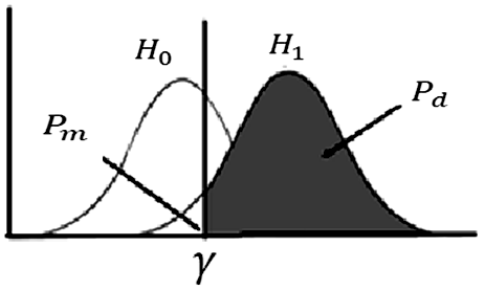

Figure: 2.4: Probabilities of detection and missed detection

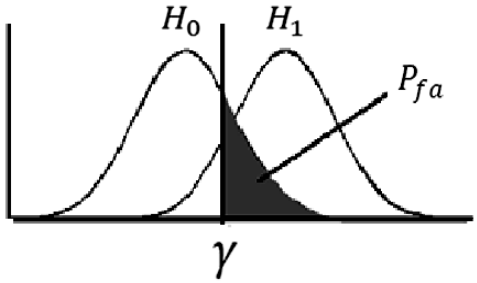

Figure: 2.5: Probability of false alarm

In the context of opportunistic DSA of the wide-band spectrum, the P_d measures the protection of primary transmission from interference due to secondary usage. While P_{fa} measures the level of opportunistic use of wide-band spectrum for a CR user. It is required that P_d is kept high and P_{fa} is kept low. But it is not possible to minimize both probabilities. A good decision criterion would be to minimize P_{fa} and P_d is kept above a certain level.

Both the probabilities depend on the value of threshold γ and the number of samples of the wide-band signal which is being sensed by CR. A trade-off occurs between the two probabilities in selection of number of samples and the sensing delay. Enough number of samples increase the accuracy of the decision about the spectral utilization at cost of sensing delay.

An overview of performance of some conventional spectrum sensing techniques using CR has been discussed below:

2.3.1 Matched Filtering

One of the well-known techniques to identify the signal pattern is matched filter detection [31]. In the presence of additive stochastic noise, the matched filter acts as an optimal linear filter to maximize the SNR. Figure 2.6 depicts the block diagram of a matched filter. The signal $\boldsymbol{r}(t)$ received by secondary user is fed to the matched filter and is expressed mathematically as

$$\mathbf{r}(\mathrm{t}) = \mathbf{hs}(\mathrm{t}) + \mathbf{n}(\mathrm{t}) \tag{2.1}$$

where $\mathbf{r}(\mathrm{t})$ is the signal received by cognitive user, $\mathbf{s}(\mathrm{t})$ is the transmitted signal transmitted, $\mathbf{n}(\mathrm{t})$ represents the AWGN noise, and $\mathbf{h}$ is the amplitude gain of the channel. The primary user is inactive if $\mathbf{s}(\mathrm{t})$ is 0. The matched filter works as if the received signal $\mathbf{r}(\mathrm{t})$ is convolved with the time-reversed version of the transmitted signal given as

$$\mathbf{r}(\mathrm{t}) \otimes \mathbf{s}(\mathrm{T} - \mathrm{t} + \tau) \tag{2.2}$$

where T is the symbol time duration and τ is the shift in the primary signal.

The output of the matched filter obtained is compared with a threshold γ in order detect the presence of the primary transmission in the spectrum.

The matched filter based sensing requires the prior knowledge of the transmitted signal such as modulation type, order, the pulse shape, and the packet format. The CRs have to store a perform synchronization according to the primary transmission which is the most cumbersome part of demodulation.

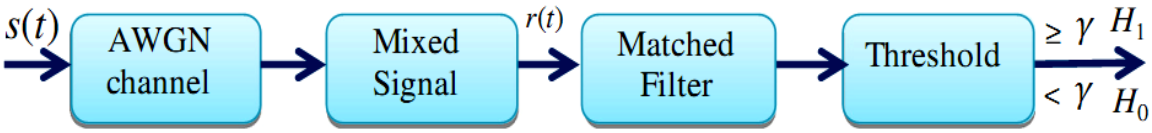

Figure: 2.6: Matched filter based spectrum sensing

The synchronization can be achieved because most primary users have pilots, preambles, synchronization words, or spreading codes that determine the coherent detection [32].

The probability of detection, P_d, and false alarm, P_{fa}, of a matched filter are given [33] as

$$P_d = Q\left(\frac{\gamma - E}{\sigma_n \sqrt{E}}\right) \tag{2.3}$$

$$P_{fa} = Q\left(\frac{\gamma}{\sigma_n \sqrt{E}}\right) \tag{2.4}$$

where Q is the Gaussian complexity distribution function, E is the energy of the received signal, and σ_n^2 is the noise variance.

2.3.2 Energy Detection

When enough information about the primary signal is not available then matched filter based sensing is not effective. In this case if the secondary user can receives the information about the power of the transmitted signal and the power of the random Gaussian noise, then energy detection based spectrum sensing is a better choice [32] for spectrum sensing.

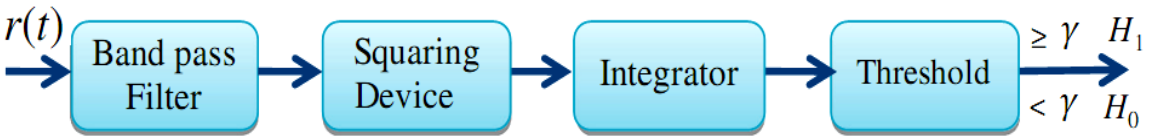

Figure: 2.7: Energy detection based spectrum sensing

Figure 2.7 depicts the block diagram for energy detection. In energy detection based spectrum sensing the power of the received signal **r**(t) is estimated by squaring and integrating the output of a band pass filter of bandwidth W over an interval T. The estimated value is compared with a threshold γ in order to detect the presence of the primary signal [34].

One of the major drawbacks of energy detection based spectrum sensing is that the performance degrades in the presence of high noise power. Since this detection scheme cannot differentiate between signal and noise power, probability of false alarm is higher at low SNR values [23].

The probability of detection, P_d, and probability of false alarm, P_{fa}, of energy detection over the AWGN channel are approximated in [32] as

$$P_d = \mathcal{Q}_m\left(\sqrt{2\boldsymbol{\Upsilon}}, \sqrt{\gamma}\right) \tag{2.6}$$

$$P_{fa} = \frac{\Gamma\left(B_E, \frac{\gamma}{2}\right)}{\Gamma(B_E)} \tag{2.7}$$

where $\Gamma(\cdot)$ and $\Gamma(\cdot,\cdot)$ are complete and incomplete gamma functions, respectively. $\mathcal{Q}_m(\cdot,\cdot)$ is the generalized Marcum Q-function, $\boldsymbol{\Upsilon}$ is the instantaneous SNR, B_E is the time bandwidth product, and γ is the decision threshold of the energy detector.

2.3.3 Cyclo-stationary Feature Detection

Commonly the primary signals can be categorized as periodic waveforms similar to cyclo-stationary feature based waveforms like sine wave carriers, pulse trains, repeating spreading, hopping sequences, and cyclic prefixes and can be c [32]. This feature is advantageous in spectrum sensing, when a secondary user detects the primary modulated waveform in the presence of random stochastic noise on the basis of periodic statistics like the mean and the autocorrelation of the primary waveform [34], as shown in Figure 2.8.

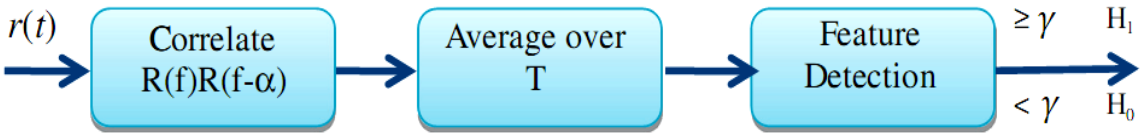

Figure: 2.8: Cyclo-stationary based spectrum sensing

The probability of detection, P_d and probability of false alarm, P_{fa} of one-order cyclostationary based spectrum sensing in AWGN channel are given by [35]

$$P_d = 1 - \left[1 - Q_m\left(\frac{\sqrt{2\Upsilon}}{\sigma_n}, \frac{\gamma}{\delta_A}\right)\right]^L \tag{2.8}$$

$$P_{fa} = 1 - \left[1 - e^{-\frac{\gamma^2}{2\delta_A^2}}\right] \tag{2.9}$$

where $\delta_A^2 = \sigma_n^2/(2Ns + 1)$ in which Ns is the number of samples for detection and L is the number of diversity branches.

Different metrics analyze the performance of the spectrum sensing algorithms. Some of these include bandwidth, resolution and real time sensing capability. Bandwidth includes

the range of spectrum that a CR will sense. Resolution is the smallest step out of bandwidth of spectrum that is quantized. Real-time sensing capability of a CR is the time in which it reliably senses the spectrum and makes adaptive decisions based on that observation of its environment and surroundings. In a wireless channels, these are time-variant characteristics in general. Thus CR must not introduce latency while sensing the spectrum, otherwise interference might occur in the transmission of the primary users. In a sensing algorithm, a trade-off occurs between the three metrics. A sensing algorithm is designed such that there is an optimized trade-off.

Analyzing the sensing algorithms, based on above mentioned metrics, both energy detection and feature based detection consisting of matched filtering and cyclo-stationary algorithms have advantages and disadvantages. In general, the feature based detection outperforms energy detection in sensing reliability and sensing convergence time. However feature based detection requires the information about characteristics of the primary users signal. Also the performance of energy detection is poor at low SNR, while that of feature based sensing performs well at low SNR.

2.4 Co-operative Spectrum Sensing

In wireless communication, the signal undergoes fading and the fluctuations in the amplitude of the signal that occur during transmission of the signal, lowers the signal strength. Fading can be slow fading or fast fading. When slow fading occurs, it does not cause significant fluctuations to the signal strength because it is frequency independent fading. Fast fading can cause significant change in the signal strength for small changes in location, because of its dependency on the frequency [5-6]. Thus to make spectrum sensing more reliable and overcome the fading problem, co-operation among the

cognitive users is a proposed solution. Information obtained while sensing the spectrum is shared between the cognitive users, to increase the efficiency of spectrum and reduce any risk of interference caused to the transmission of primary users. The spectrum is sensed collectively rather than individually. Co-operation in spectrum sensing relies on the varying signal strength at different locations. Co-operative spectrum sensing can be centralized or distributed depending upon the method of sharing spectrum information among the cognitive users [5-6]

2.4.1 Centralized Sensing

In centralized spectrum sensing, all cognitive nodes sense the spectrum and update the information about their individual sensing to the central unit [36]. The central unit identifies the available spectrum and then broadcasts the information to the CRs and controls he transmission from each CR node.

2.4.2 Distributed Sensing

In distributed sensing, the CR nodes share the information among each other and there is no role of a central unit in sharing the information and controlling the transmission of any CR node [36].

Distributed sensing is more effective compared to centralized sensing in the sense that it does not require a backbone infrastructure; CR nodes make decisions on their own observation; so it is less costly.

2.5 Wide-band Spectrum Sensing using CR

When spectrum sensing techniques are explored in wide-band regime, one usually infers that the propagation of the signal takes place over ideal free space. The free space model refers to the region between the transmitting and receiving antennas as being free of all

obstacles that might absorb or reflect RF energy. For such ideal propagation model, the received signal power is predictable.

In practical channels like Rayleigh fading channels, signal propagation takes place in the atmosphere and near the ground such that the signal follows the phenomenon of multi-path propagation; it travels from transmitting antenna to receiving antenna over multiple reflective paths. Multi-path propagation can affect the power of signal propagated; fluctuations occur in the received signal's amplitude, phase, and angle of arrival. This effect is called multi-path fading. The performance of the system model is affected due to multi-path fading in practical channels. So a more comprehensive study of the performance of the wide-band spectrum sensing algorithms in practical channels is needed. An initiative step has been taken in this regime to introduce a Bayesian inference approach in CS algorithm for wide-band signals that follow a Rayleigh distribution.

As it has been discussed earlier in section 1.2 and section 1.3, the secondary users can sense the wide-band spectrum and identify the vacant slots/holes in it for communication and signal transmission. The conventional way to detect the spectral holes in the wide-band spectrum using CR is channel-by-channel scan. An RF front end is implemented with a bank of tunable narrow band-pass filters that detects the occupancy of each channel by measuring the energy of the signal being transmitted in that channel.

However for wide-band spectrum sensing, the tuning of numerous RF components makes it complex as well as costly. Some alternative techniques have been proposed in the literature to facilitate wide-band spectrum sensing.

In [37], a wide-band spectrum sensing approach has been proposed in which the aggregate opportunistic throughput is maximized based on the restrictions applied on the

interference caused to the transmission of the primary user. In this approach, energy detection is performed at each narrow band channel and compared with a predefined threshold. The threshold levels obtained for each channel provide solution to optimization problem such that aggregate throughput for CR is maximized. The co-operative approach is followed in which CRs share their sensing information in order to make wide-band spectrum sensing more reliable and counter any severe effect of fading.

Another approach of wide-band spectrum sensing based on Maximum Likelihood (ML) estimation of the signal and noise power has been proposed in [38] to detect the unoccupied channels. In this method, iterative asymptotic ML estimation is simplified such that efficient least square is estimated. The performance of the algorithm is evaluated for different number of channels and for different SNRs.

To further investigate faster sensing methods, CS approach has been introduced for wide-band spectrum sensing and detection [39-40].

2.5.1 Compressive Sensing (CS) Theory

According to Nyquist theorem, a signal can be exactly recovered from a set of uniformly spaced samples only if the sampling/Nyquist rate is two times greater than the highest frequency present in the signal of interest.

For a signal $\mathbf{x} \boldsymbol{\epsilon} \mathbb{R}^{\boldsymbol{N}}$**,** the Nyquist sampling can be performed using an identity matrix $\boldsymbol{\Phi} = \mathbf{I}_{N \times N}$ to get $N \times 1$ measurement vector **y,** as shown in Figure 2.9.

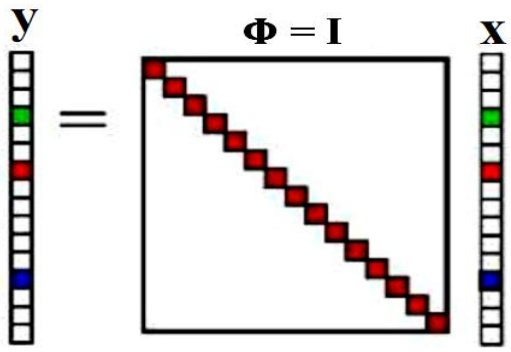

Figure: 2.9: Nyquist sampling

However, in emerging applications and technologies, the required Nyquist rate is too high. This renders the process too complicated and costly; since it becomes physically impossible to build up device that are capable of acquiring such higher Nyquist rates.

To deal with such high-dimensional data, one method is compressive sampling of the signal. Compressive sampling of the signal aims to find the most concise representation of the signal such that a target level of distortion is acceptable. CS is a sampling method in which lesser number of measurements is required to recover the spars signal compared to those required in traditional Nyquist sampling method.

Intensive research is being made in CS, because in real world wireless or mobile communication, the signals posses very few non-zero elements. Such signals which contain noise more than information in them are known as sparse signals. Wide-band signals fall into the category of sparse/compressive signals, since there is more noise added to the signal elements compared to those signal elements which contain useful information. Sensing of wide-band signals faces technical challenges, when radio front end requires a bank of narrow band-pass filters that are tuned to specific frequency range. Too large number of RF components and tuning range requirement render it impossible.

An alternative way is to adopt a wide-band circuit that utilizes a single RF chain that is connected to high speed digital signal processor. Such circuit will search over multiple frequency bands at a time, but this requires very high sampling rates that are equal to or above the Nyquist rate. Also the requirement of faster sensing process, renders fewer measurements to be achieved from the received signal, which may not provide sufficient statistics for linear reconstruction of the signal. CS aims at providing faster sampling of the wide-band signal at a sampling rate that is far below Nyquist rate. The CS approach promises to provide enough statistics from the measurements obtained from the received signal, that makes sure an accurate recovery of the signal is possible from them.

In CS scenario, a wide-band signal $\mathbf{x} \in \mathbb{R}^{N}$ can be represented in the form of a basis such as

$$\mathbf{x} = \mathbf{\Psi r} \tag{2.11}$$

where $\mathbf{\Psi} \in \mathbb{R}^{\mathbf{N}\times\mathbf{N}}$ is an orthonormal basis and $\mathbf{r} \in \mathbb{R}^{\mathbf{N}}$ attributes the sparsity level of signal $\mathbf{x}$ as

$$\|\mathbf{r}\|_{\mathbf{0}} = K \ll N \tag{2.12}$$

Sensing/sampling of such wide-band signals would be costly and complex as well, if Nyquist sampling method is used. The sparsity feature of the wide-band signal allows throwing away less useful information instead of sampling all N values of the signal.

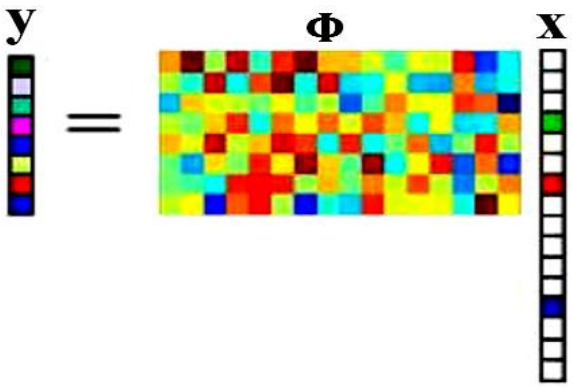

Figure: 2.10: Compressive sampling

Instead, we can recover the signal **x** from few projections onto incoherent measurement vector **y**. A sensing matrix $\mathbf{\Phi} \in \mathbb{R}^{M \times N}$ provides us with the measurement vector **y** such that

$$\mathbf{y} = \mathbf{\Phi x} + \mathbf{n} \tag{2.13}$$

where the additive noise vector $\mathbf{n} \in \mathbb{R}^{M}$ drawn from *i.i.d.* zero-mean Gaussian noise distribution $\mathcal{N}(0, \sigma_n^2 \mathbf{I}_M)$, where σ_n^2 represents the variance of noise distribution and $\mathbf{I}_M$ is identity matrix of order $M \times M$ and the number of measurements $M \ll N$ as shown in Figure 2.10.

In conventional Nyquist sampling method, $\mathbf{\Phi}$ is the $N \times N$ identity matrix; while in CS $\mathbf{\Phi}$ is generally $M \times N$ matrix, such that the coherence/correlation between the sensing matrix $\mathbf{\Phi}$ and the basis matrix $\mathbf{\Psi}$ is very small, given by

$$\mu(\mathbf{\Phi}, \mathbf{\Psi}) = \sqrt{\mathbf{N}} \cdot \max_{1 \le i,j \le N} \left| \langle \mathbf{\Phi}_i, \mathbf{\Psi}_j \rangle \right| \tag{2.14}$$

The largest correlation between the two matrices determines the coherence between the two matrices. CS requires both the sparsity feature and minimum coherence factor between the sensing matrix and the basis matrix, to recover the signal accurately.

The signal **x** is decoded using the measurement vector **y** and the sensing matrix **Φ**. Since the decoding process is ill-posed inverse problem where number of measurements are lesser than number of unknowns, the sparsity factor of the signal enables us to decode **x** from $M \ll N$ measurements. Decoding **x** relies on optimization technique, where those sparsest coefficients of **r** are examined to satisfy with the measurement vector **y** elements. If there is sufficient number of measurements and **r** is strictly sparse, then **r** is the solution to ℓ_0-minimization given as

$$\hat{\mathbf{r}} = \arg\min_{\mathbf{r}} \|\mathbf{r}\|_0 \tag{2.15}$$

where $\hat{\mathbf{r}}$ is the recovered **r**, which comprises to recover **x** provided $\mathbf{x} = \mathbf{\Psi r}$. However solution to ℓ_0-minimization is NP-hard problem [11-12].

So CS theory reveals that ℓ_1-minimization yields computationally tractable solution [13-14], when only ℓ_1 sparsest coefficients are needed that satisfy with the measurement elements, and is given as

$$\hat{\mathbf{r}} = \arg\min_{\mathbf{r}} \|\mathbf{r}\|_1 \tag{2.16}$$

2.5.2 Bayesian Compressive Sensing (BCS)

The CS method can be further simplified by using Bayesian inference, provided the system model supports Bayesian approach [15-16]. The Bayesian inference provides solutions that are conditional on the observed data; it estimates a full probability model, where probability distributions are associated with parameters or hypotheses. In this approach, the decoding process of the signal is considered as a MAP estimation problem given as

$$\hat{\mathbf{x}} = \arg\max_{\mathbf{x}} f_{\mathbf{X}}(\mathbf{x}|\mathbf{y}) \qquad s.t.\ \mathbf{E}\|\mathbf{\Phi x} - \mathbf{y}\| \leq \epsilon \tag{2.17}$$

where $\hat{\mathbf{x}}$ is the signal recovered via BCS, $f_{\mathbf{X}}(\mathbf{x}|\mathbf{y})$ is the conditional PDF of **x,** $\mathbf{E}[\cdot]$ the expectation operator and $\boldsymbol{\epsilon}$ is a user defined parameter for tolerance in error.

BCS approach offers solution with low computational cost for the recovery of the signal. In BCS approach, the conditional PDF of the signal vector is obtained via BP, in which the messages are exchanged between the signal nodes and the measurement vector nodes. BP is a sum-product algorithm which estimates the marginal distributions for random variables through exchanging messages among the factor graphs [42-43].

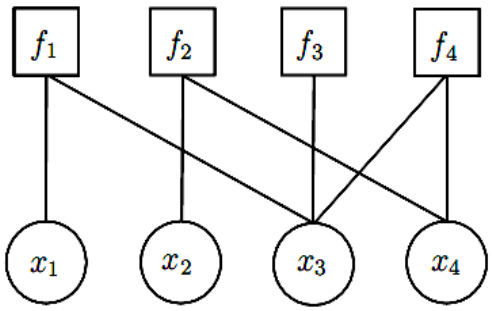

Figure: 2.11: Factor graph illustration

A global function $F(x_1, x_2, x_3, \cdots, x_n)$ can be factorized as

$$F(x_1, x_2, x_3, \cdots, x_n) = \prod_i f_i(\mathbf{X}_i) \tag{2.18}$$

where $f_i(\mathbf{X}_i)$ is a local function, which has $\mathbf{X}_i = (x_1, x_2, x_3, \cdots, x_n)$ arguments. This factorization can be represented as factor graphs as shown in Figure 2.11. Factor graphs consist of nodes and edges. Nodes in a factor graph can be variable nodes that represent independent variables or factor nodes that represent local functions, while the edges connect a factor node f to a variable node $\mathbf{x}$ if and only if f is a function of $\mathbf{x}$. BP

algorithm works on the principle of exchanging messages between variable and factor nodes in a factor graph. A-priori information from the variable nodes is received by the function node that is connected to it through an edge. This information is then used to estimate the a-posteriori probabilities for the connected variable nodes and this estimate is passed back to the variable nodes. Using the updated information, the variable nodes calculate their new a-priori probabilities. The message that is passed along the edge from the variable node x to factor node f, is denoted by $\mu_{x\to f}(x)$. It is updated by taking the product of all the messages received by the variable node x from other edges connected to it:

$$\mu_{x\to f}(x) = \prod_{u\in n(x)\backslash\{f\}} \mu_{u\to x}(x) \tag{2.19}$$

where $n(x)\backslash\{f\}$ represents all factor nodes connected to x excluding factor node f. While, the message that is passed along the edge from the factor node f to variable node x, is denoted by $\mu_{f\to x}(x)$. It is updated by multiplying the local function f with the product of all the messages received by the function node f from all other edges connected to it. The result is then marginalized such that it becomes a function of x only:

$$\mu_{f\to x}(x) = \sum_{\sim\{x\}} \left(f(\mathbf{X}) \prod_{v\in n(f)\backslash\{x\}} \mu_{v\to f}(v) \right) \tag{2.20}$$

where $\mathbf{X} = n(f)$ represents set of all variable nodes connected to f and $\sim\{x\}$ represents set of all variables nodes connected to f excluding x. When BP converges, the marginal distribution $f(x)$ for the variable node x is computed by taking the product of all the messages received by x that is

$$f(x) = \prod_{u \in n(x)} \mu_{u \to x}(x) \tag{2.21}$$

where $n(x)$ represents all factor nodes connected to x.

A BP algorithm can be implemented as tree factor graph or cyclic factor graph. BP algorithm implemented as a tree factor graph converges exactly after number of iterations that is equal to the depth of the tree, and the marginal distributions are estimated. In cyclic factor graph implementation, the cycle/loop ends at the same node from where it started. Though the BP algorithm does not possess natural termination, but it needs to be stopped after specified number of iterations, when minor improvements occur in messages [44-46].

Numerical results for cyclic factor graph BP algorithm implementation show that it achieves near-optimal results even without convergence.

2.5.3 Prior Models for Belief Propagation

The success of BP propagation algorithm depends upon the appropriate choice of the system model and the prior model that matches with the system model. Depending upon the signal model and the channel existing, some prior models have been discussed below.

2.5.3.1 Two State Gaussian Mixture

The two-state Gaussian mixture distribution [41] has been introduced in [15-16] to model the prior for a sparse signal element in an AWGN channel. Let **x** be a sparse signal of dimension $1 \times N$. It contains $K \ll N$ signal elements with more information compared to rest of the signal elements which contain lesser information or simply the Gaussian noise that is added to it. Each signal element can be associated with a state variable from a state

vector $\mathbf{v} = [\mathrm{v}_1, \mathrm{v}_2, \mathrm{v}_3, \cdots, \mathrm{v}_\mathrm{n}]$, where $\mathrm{v}_\mathrm{i} \in \{0, 1\}$, for $\mathrm{i} = 1, 2, 3, \cdots, \mathrm{N}$. The large signal element which contains more information is associated with a 'high' state variable i.e. 1, while a small signal element that contains less information is associated with a 'low' state variable i.e., 0. Each state variable is then associated with a probability function $p(\mathrm{x}_\mathrm{i})$ for each element, where $\mathrm{i} = 1, 2, 3, \cdots, \mathrm{N}$. So the 'high' state variable for each large signal element is associated with a high variance zero mean Gaussian distribution given by

$$f_{\mathbf{X}}(\mathbf{x}|\mathbf{v} = 1) \sim \mathcal{N}\left(0, \sigma_{\mathbf{x}_1}^2\right) \tag{2.22}$$

where $\mathcal{N}\left(0, \sigma_{\mathbf{x}_1}^2\right)$ represents Gaussian distribution with mean 0 and variance $\sigma_{\mathbf{x}_1}^2$. The 'low' state variable for small signal element is associated with a low variance zero mean Gaussian distribution given by

$$f_{\mathbf{X}}(\mathbf{x}|\mathbf{v} = 0) \sim \mathcal{N}\left(0, \sigma_{\mathbf{x}_0}^2\right) \tag{2.23}$$

where $\sigma_{\mathbf{x}_1}^2 > \sigma_{\mathbf{x}_0}^2$.

The complete prior model for the sparse signal in AWGN channel is stated as

$$f_{\mathbf{X}}(\mathbf{x}) = \prod_{\mathrm{i}=1}^{\mathrm{N}} q\mathcal{N}\left(0, \sigma_{\mathbf{x}_i}^2\right) + (1 - q)\mathcal{N}\left(0, \sigma_{\mathbf{x}_i}^2\right) \tag{2.24}$$

where $q = \frac{K}{N}, q \in [0, 1)$ is the sparsity rate to represent the probability of $K \ll N$ large signal coefficients. The messages passed in BP are fully parameterized via $\sigma_{\mathbf{x}_1}^2$, $\sigma_{\mathbf{x}_0}^2$ and q.

2.5.3.2 Gaussian-Spike Prior Model

Recently in [47-49], BP algorithm has been devised for such signal models as sparse vectors which are deterministic realization of Gaussian signals. For such signal models and strictly sparse signals, the spike distribution has been introduced as a prior

distribution for the small signal coefficients. The sparsifying Gaussian-Spike prior model for such signal model is also known as spike-and-slab prior model and it is given as

$$f_{\mathbf{X}}(\mathbf{x}) = q\mathcal{N}(0, \sigma_{\mathbf{x}}^2) + (1-q)\delta(\mathbf{x}) \tag{2.25}$$

Where $\delta(\mathbf{x})$ is Dirac distribution, such that there is a non-zero value between $\mathbf{x} \in [0-, 0+]$ such that $\int \delta(\mathbf{x})dx = 1$.

2.5.3.3 Rayleigh-Spike Prior Model

Above Gaussian prior models represent the signal models that are propagated in free space propagation models or AWGN channels. Such channels refer to the signal propagation in a region between the transmitting and receiving antennas that is free of all obstacles that might absorb or reflect RF energy. In such ideal propagation model, the received signal power is predictable.

However in wireless communication and realistic scenarios, the signals are not propagated in free-space model as discussed in section 2.5. Fading is an inherent feature of real-time propagation models. The signals that are propagated in practical channels like Rayleigh channels undergo reflection, refraction and diffraction, and the signal's amplitude is varied due to multipath effect. The multipath effect affects the signal power. The signal processing techniques perform differently for the Rayleigh faded signals propagated in Rayleigh channels compared to those propagated in AWGN channels. Thus it is inadequate to describe a practical channel like Rayleigh fading channel using a free-space propagation model.

When BCS algorithm is being used for detection of wide-band signal that is propagated in Rayleigh fading channel, the decoding of the Rayleigh faded signal via BP algorithm is

different from the signal propagated in AWGN channel. It is appropriate to choose such prior model that best matches with the properties of the signal model. For Rayleigh faded signal models, we have introduced Rayleigh distribution as the prior distribution for large signal elements with variance $\sigma_{\mathbf{x_1}}^2$ that is given by

$$f_{\mathbf{X}}(\mathrm{x_i}|\mathrm{v_i} = 1) = \left(\frac{\mathbf{x}}{\sigma_{\mathbf{x_1}}^2}\right) e^{\left(\frac{-x^2}{2\,\sigma_{\mathbf{x_1}}^2}\right)} \tag{2.26}$$

The small signal elements can be described by Spike distribution as in Gaussian-Spike prior model. Thus the Rayleigh-Spike prior model can be given as

$$f_{\mathbf{X}}(\mathbf{x}) = q\left(\frac{\mathbf{x}}{\sigma_{\mathbf{x_1}}^2}\right) e^{\left(\frac{-x^2}{2\,\sigma_{\mathbf{x_1}}^2}\right)} + (1-q)\delta(\mathbf{x}) \tag{2.27}$$

Such types of priors have been used for strictly sparse signal models [50-51], since the prior easily characterizes the signals by $\sigma_{\mathbf{x_1}}^2$ and q factors. Since the elements in **x** are assumed to be $i.i.d.$ Rayleigh distributed, the prior density represents each i^{th} signal coefficient independently.

2.6 Summary

In this chapter, different concepts related to wideband spectrum sensing and CR, have been discussed. Different conventional techniques used to sense the spectrum have been studied. The disadvantages in using conventional methods for wideband spectrum sensing have also been discussed. The fading phenomenon in wide-band signals has been overviewed to improve the performance of signal processing in real-time scenarios. CS and BCS via BP algorithms have been explored for wideband spectrum sensing.

Chapter 3

COMPRESSIVE SENSING AND DETECTION OF WIDEBAND SPECTRUM USING CR

3.1 Introduction

In this chapter, CS techniques for wideband spectrum sensing using CR are proposed. A CS technique is proposed that estimates the wideband spectrum such that time delay and sampling rate is decreased. In this technique specific portions of the time samples of the signal are ignored while the signal is being sensed compressively. The sampling rate can be decreased by choosing elements of sensing matrix randomly for CS. Compressive detection is also performed to detect the vacant channels in the spectrum. In this approach, wideband signal is fed into wideband band-pass filters such that energy of each channel in the wideband signal is estimated at the each filter output compressively using l_1-minimization. Then energy detection is performed over the energy vector obtained and the occupancy of the channel is decided by comparing it to already defined energy threshold level.

3.2 Problem Statement

Consider a wideband spectrum of WHz such that it has N number of channels, where each channel has a bandwidth BHz. To sense this wideband spectrum, a wideband antenna connected to the CR node, receives the time-domain signal $\mathbf{x}(t)$, such that for a T time interval, the signal is sampled at a sampling period of T_0

$$\mathbf{x_t} = \{\mathbf{x}(\mathrm{t})\}|_{\mathrm{t}=nT_0}, \qquad n = 1, 2, 3, \cdots, N \tag{3.1}$$

where $N = T/T_0$ represents the number of samples of $\mathbf{x_t}$ for the time interval $[0, T]$. The time domain signal $\mathbf{x_t}$ is represented in frequency domain as $\mathbf{x_f} = \mathcal{F}\{\mathbf{x_t}\}$. It is given by

$$\mathbf{x_f} = \mathbf{F}_N \mathbf{x_t} \tag{3.2}$$

where

$$\{\mathbf{F}_N\}_{i,k} = \frac{1}{\sqrt{N}} e^{\frac{j2\pi(i-1)(k-1)}{N-1}}, \quad i, k = 1, 2, 3, \cdots, N \tag{3.3}$$

The wideband spectrum has holes or vacant spaces in it, where no transmission is taking place. The problem is to identify those spectral holes in the received signal.

3.3 Wideband Spectrum Reconstruction via CS with Reduced Delay and Complexity

In this section, we propose CS algorithm for estimation of wideband spectrum such that the delay in sensing time is reduced by using fewer samples of time domain wide-band signal. We consider that a wideband time domain signal $\mathbf{x}(t)$ is sampled at Nyquist rate such that the frequency domain signal $\mathbf{x_f}$ is a sparse signal; only $K \ll M$ signal coefficients posses most of the data i.e., large signal coefficients. The rest of the signal coefficients $M - K$ are small signal coefficients in a sense that they posses only noise elements or smaller data compared to K large signal coefficients. Thus K denotes the sparsity level of the wideband signal.

The measurements of the signal are obtained via $M \times N$ sensing matrix $\mathbf{\Phi}$ to form a $M \times 1$ measurement vector $\mathbf{y}$ given by

$$\mathbf{y} = \mathbf{\Phi x_t} \tag{3.4}$$

Since the number of measurements M is quite less than the number of samples N of the signal. The frequency samples of the signal are recovered using ℓ_1-norm minimization given by

$$\hat{\mathbf{x}}_f = \arg\min_{\mathbf{x}_f} \left\| \mathbf{x}_f \right\|_1, \quad \text{subject to } \mathbf{y} = \mathbf{\Phi}\mathbf{F}_N^{-1}\mathbf{x}_f \tag{3.5}$$

The complexity of conventional algorithms for sensing of wideband signal can be reduced via CS, in which fewer linear combinations or measurements are used to recover the signal.

In [39] a full random sensing matrix **Φ,** is chosen such that all $N = T/T_0$ samples of the signal are collected for a total time interval T. The sensing delay can be further reduced by selecting the matrix elements freely such that only a fraction of time interval T i.e., T_s seconds are used to collect the samples. The sensing time is decreased such that $S = \frac{T_s}{T_0}, S < N$ samples of time domain signal $\mathbf{x}_t$ are collected to generate the measurement vector **y.** Initial S samples are gathered such that first S columns of sensing matrix **Φ** are randomly chosen from a Gaussian distribution. The rest of $N - S$ columns are all set to zero, given as

$$\mathbf{y} = \mathbf{\Phi}\mathbf{x}_t = \left[\mathbf{S}\middle|\mathbf{0}_{M\times(N-S)}\right]\mathbf{x}_t = \mathbf{S}\mathbf{x}_t^S \tag{3.6}$$

where **S** is a $M \times S$ random matrix and $\mathbf{x}_t^S$ consists of initial S time samples of $\mathbf{x}_t$**.** This leads to faster sensing. Within $T_s = ST_0$ seconds, the cognitive system starts to recover $\mathbf{x}_f$ and consequently the spectral holes can be identified as shown in figure 3.1.

Another approach to reduce the time aperture using S columns can be considered by padding $N - S$ zero columns within the sensing matrix **Φ** such that reduced number of samples e.g., $\frac{S}{N} = \frac{2}{3}$ or $\frac{4}{5}$ etc are collected when one out of three or one out of four

columns are chosen to be zero respectively. Thus sampling rate is reduced further up to $\frac{2}{3}$ or $\frac{4}{5}$ of Nyquist rate. Better performance of CS algorithm can be achieved in terms of reducing the processing delay in wideband sensing for practical channels as shown in figure 3.2.

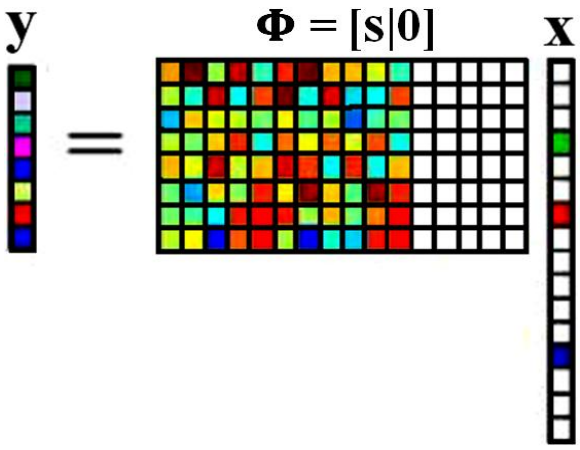

Figure: 3.2: Compressive sampling by inserting columns of zeros in sensing matrix

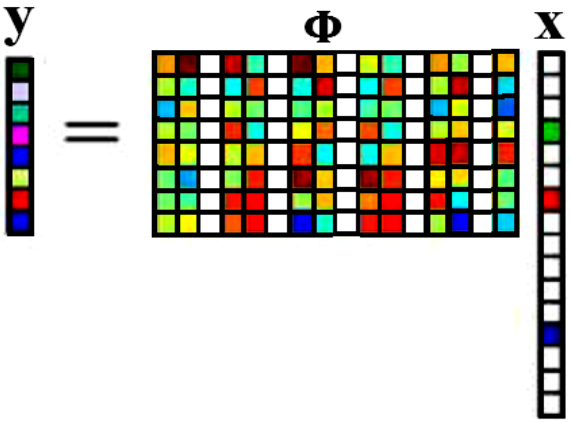

Figure: 3.3: Compressive sampling by distributing columns of zeros in sensing matrix

A CR functions to estimate the vacant spaces in a wideband spectrum which can be utilized for secondary usage. For this purpose, it has to estimate the energy level in each

channel of the spectrum. As long as the adequate detection of vacant channels is achievable, accurate recovery of the spectrum is tolerable.

To estimate the spectrum of the wideband signal accurately, the number of measurements M must satisfy the following inequality [52]

$$M \geq cK \log(N/K) \tag{3.7}$$

where K is the sparsity level of the signal. Based on this inequality, we can reconstruct the spectrum using smaller number of time samples with M even lower than threshold needed for $S = N$. However number of time samples cannot be lowered further than S, since then the reconstruction would not be possible with such less information of the signal input.

3.4 Wideband Signal Detection via CS Using Cognitive Bayesian Energy Detector

In this section, the CR is used to detect the occupied/unoccupied slots in the wide-band signal using CS approach. The CR can adopt a Bayesian energy detector to decide about the occupancy of the channel using a threshold energy level. It utilizes the information of the estimated spectrum via CS, sums up the components of the estimated signal in each frequency band and calculates the energy residing in each frequency band i.e. e_i. For set of all frequencies sampled in ith channel i.e., Ω_i, the energy residing in each frequency band is given by

$$e_i = \sum_{j \in \Omega_i} \left|\mathbf{x}_{f,j}\right|^2, \quad i = 1, 2, 3, \cdots N \tag{3.8}$$

Thus the energy vector of the received signal can be defined as

$$\mathbf{e} = [e_1, e_2, e_3, \cdots, e_N] \tag{3.9}$$

Since most of the frequency bands are unoccupied in a wide-band spectrum, the energy vector is a sparse vector.

In a CR energy detector, M wide-band filters are connected to each node such that the transfer function for m^{th} channel is given by:

$$h_m(f_i) = [\mathbf{\Phi}]_{m,i}, \qquad m = 1, 2, 3, \cdots, M, \;\; i = 1, 2, 3, \cdots, N \tag{3.10}$$

where $\mathbf{\Phi}$ is $M \times N$ matrix assigned to each CR node. The signal is fed to the M wide-band filters such that the output obtained at the m^{th} filter is given by

$$\mathbf{z_m} = \text{conv}(\mathbf{x_t}, \mathbf{h_m}) \tag{3.11}$$

where $\text{conv}(\cdot,\cdot)$ denotes the convolution operation and $\mathbf{h_m}$ denotes the impulse response sequence of the m^{th} filter. The energy of the output signal obtained at m^{th} filter node is estimated as

$$y_m = \mathbf{z_m^H z_m}, \quad m = 1, 2, 3, \cdots, M \tag{3.12}$$

where $(\cdot)^H$ is conjugate transpose of a matrix.

The energy vector $\mathbf{y}$ is measured as

$$\mathbf{y} = [y_1, y_2, y_3, \cdots, y_M]^T \tag{3.13}$$

where $(\cdot)^T$ is transpose of a matrix.

For a constant frequency response throughout each channel, the energy at the output of m^{th} filter is given by

$$y_m = \sum_{i=1}^{N} |h_m(f_i)|^2 e_i, \quad m = 1, 2, 3, \cdots, M \tag{3.14}$$

For a random matrix **Φ**, the square absolute values of the elements can be obtained from equation (3.15) to form a matrix **H** such that

$$\mathbf{H} = \begin{bmatrix} |h_1(f_1)|^2 & |h_1(f_2)|^2 & \cdots & |h_1(f_N)|^2 \\ |h_2(f_1)|^2 & |h_2(f_2)|^2 & \cdots & |h_2(f_N)|^2 \\ \vdots & \vdots & \ddots & \vdots \\ |h_M(f_1)|^2 & |h_M(f_2)|^2 & \cdots & |h_M(f_N)|^2 \end{bmatrix} \tag{3.15}$$

Thus $M \times 1$ measurement energy vector **y** can be estimated as

$$\mathbf{y} = \mathbf{He} \tag{3.16}$$

The main goal is to estimate the length N energy vector **e** using M measurement vectors. Since, in a wide-band spectrum, most of the channels are unoccupied, the channel energy vector **e** is sparse. So compressive detection process can be established by correspondence between the filter based CR nodes design and CS theory. By proper selection of number of filters M for a CR node, the channel enrgy vector eastimation is possible from the measurement energy vector, i.e.,

$$\hat{\mathbf{e}} = \arg\min_{\mathbf{e}} \| \mathbf{e} \|_1 \quad subject\ to\ \mathbf{y} = \mathbf{He} \tag{3.17}$$

Thus each CR node reconstructs the channel energy vector **e** from measurement vector **y,** and the energy vector coefficients are compared to a threshold to decide about the occupancy of each channel.

The threshold chosen for detection process depends upon the maximum interference level allowed by the primary user. For a distance D between the primary transmitter and primary receiver and Signal-to-Interference Ratio (SIR) γ_i, the interference range for the primary receiver at distance R is given by

$$(P_p \cdot L_D) \,/\, (P_s \cdot L_R) + I_b = \gamma_i \tag{3.18}$$

where P_p is primary transmitter's power, P_s is secondary CR's transmitiing power, $I_b$is the background interference at the primary receiver and L_D is path loss at distance D, L_R is path loss at the primary receiver side.

The CR node should be capable of sensing all the signals coming from a distance $D + R$ and the signals with transmit power $P_{min} \geq (P_p \cdot L_{D+R})$. Thus for a channel with bandwidth B and $P_{min} > BN_o$, where N_o is the spectral density for noise, the threshold should be set below P_{min} and above the level noise. In this approach, the CR node will never be in the interference range for primary receiver and it can transmit as a secondary unit in the underlying channel. The information about the primary parameters I_b, γ and D should be provided by the regulating authorities or primary systems correspondents [53].

3.5 Summary

In this chapter, wide-band spectrum sensing and detection of vacant channels is performed via CS. The basis pursuit approach for CS reduces the time-aperture for spectrum sensing. This provides a solution to the latency caused due to channel-by-channel scanning of a wide-band spectrum.

Chapter 4

CS FRAMEWORK FOR RAYLEIGH FADING CHANNELS USING BAYESIAN INFERENCE APPROACH

4.1 Introduction

In this chapter, the CS via BP algorithm has been modified to represent the signal propagation in practical channels. As we have discussed earlier in chapter 1 and chapter 2, the radio waves that are transmitted in mobile communications, satellite communications and other wireless communication systems undergo the phenomenon of fading. The transmitter transmits the signal in a region which contains obstacles to absorb/reflect the RF wave. The transmitted signal travels over multiple reflective paths and degradation in its energy/power is observed. This is caused due to the multipath effect which results in scattering, reflection and diffraction of the transmitted signal. Such phenomenon of fading suggest more study of signal propagation in practical channels like Rayleigh fading channels along with signal propagation in classical AWGN channel.

As we have discussed earlier, CS facilitates the acquisition and sensing of wide-band signals at rates that are significantly lower than Nyquist rates. The CS method can be further simplified using Bayesian inference approach for the sensing and detection of wide-band signals that follow Rayleigh distribution due to Rayleigh fading channels. The system model for Rayleigh fading channel supports Bayesian approach, since the Bayesian inference provides solutions that are conditional on the observed data. The Bayesian inference approach estimates a full probability model, where probability

distributions are associated with parameters or hypotheses, such that decoding process of the Rayleigh faded signal is considered as MAP estimation problem.

The Bayesian approach for sparse signal reconstruction using Low-Density-Parity-Check (LDPC) codes [54] in channel coding motivates the use of sparse matrices for simple and fast CS signal recovery for real world applications. Iterative message passing via BP further reduced the complexity of CS algorithm [55-56].

In previous BP algorithms for CS signal reconstruction, the BP messages are treated as Gaussian probability density functions, however messages should be in accordance to the signal model.

We have proposed the usage of BCS framework for spectrum sensing in a practical wireless channel like Rayleigh fading channel. In such channels, the signal undergoes fading due to the multi-path effect. The free space propagation model assumes the signal propagation in AWGN channel, thus it is inadequate to describe a practical channel like Rayleigh fading channel using a free space model. Also the performance of the system would be different for the classic AWGN channel and the practical Rayleigh channel. In this paper, we have modified the BCS framework with appropriate priors for the decoding of the Rayleigh faded signal via BP. Our results show that when an appropriate prior is used according to the system model, the recovery of the signal improves. Also an improvement in MSE can be achieved.

4.2 Problem Formulation

In practical scenario, the wide-band signal from the transmitter travels over multiple reflective paths to the receiver. Due to multi-path fading, the envelope of the signal is

statistically described by the Rayleigh PDF. Thus practical Rayleigh fading channel will describe such system models.

In this paper, we have explored the implementation of BCS framework in Rayleigh fading channels, where the desired unknown signal follows the Rayleigh distribution.

To sense the wideband signal in Rayleigh fading channel, consider a wide-band signal $\mathbf{k}(t)$**,** such that for a time interval T, the signal is sampled at a sampling period of T_0.

$$\mathbf{k_t} = \{\mathbf{k}(t)\}|_{t=nT_0}, \quad n = 1, 2, 3, \cdots, N \tag{4.1}$$

Each signal sample in $\mathbf{k_t}$**,** i.e., $\mathbf{k_t}$(n) undergoes a Rayleigh flat fading channel with **h** vector consisting of $i.i.d.$, channel coefficients given by

$$\mathbf{h} = \{\mathbf{h}_i\}, \quad i = 1, 2, 3, \cdots, N \tag{4.2}$$

A Rayleigh faded signal vector $\mathbf{x_t} \in \mathbb{R}^{N}$ is obtained

$$\mathbf{x_t} = \mathbf{h}_i.\mathbf{k_t}(\text{n}), \quad n = 1, 2, 3, \cdots, N, \;\; i = 1, 2, 3, \cdots, N \tag{4.3}$$

The wide-band spectrum of the signal is sparse given by,

$$\mathbf{x} = \mathcal{F}(\mathbf{x_t}) = \mathbf{H}\mathbf{k_f} \tag{4.4}$$

where **H** represent the frequency domain samples Rayleigh fading channel and $\mathbf{k_f}$ is the sparse wide-band spectrum of the signal $\mathbf{k_t}$ that undergoes Rayleigh fading such that there are only $K \ll N$ non-zero coefficients. Thus the sparsity of the signal **x** is given by by some vector **r** i.e.,

$$\|\mathbf{r}\|_0 = K \ll N \tag{4.5}$$

where $\|\mathbf{r}\|_0$ represents number of non-zero coefficients in **x**. Thus the sparse Rayleigh faded signal **x** contains only K non-zero coefficients out of N samples.

The sensing/sampling of such wide-band signals would be costly and complex as well, if Nyquist sampling method is used. However the sparse nature of this Rayleigh faded signal allows us to recover the signal via CS with lesser number of measurements. A sensing matrix $\mathbf{\Phi} \in \mathbb{R}^{M \times N}$ provides us with the measurement vector **y** such that

$$\mathbf{y} = \mathbf{\Phi x} \tag{4.6}$$

such that the number of measurements $M \ll N$.

Our goal is to recover the sparse Rayleigh distributed signal **x**.

Since the number of measurements M is lesser than the number of unknown signal elements N, we suggest BCS solution for the recovery of the signal. We assume that $i.i.d.$ signal elements of sparse Rayleigh distributed signal **x** can be independently related to the support set $supp(\mathbf{x})$ with sparsity rate $q \in [0, 1)$, such that state vector **s** can be associated with each element based upon its association with $supp(\mathbf{x})$ as

$$s_i = \begin{cases} 1 & if\ i \in supp(\mathbf{x}) \\ 0 & otherwise \end{cases} \quad for\ i \in \{1, 2, 3, \cdots, N\} \tag{4.7}$$

In the following sections, we proposed our system model for BCS framework and then we discussed the solution approach for the recovery of the Rayleigh faded signal **x** via BCS.

4.3 Proposed System Model

In this section we discuss the graphical representation of the sensing matrix **Φ** and the prior model to be used in the BCS framework for Rayleigh fading channels.

4.3.1 Sparse Sensing Matrix

To encode the signal **x** we consider a sparse-binary sensing matrix $\mathbf{\Phi} \in \{0,1\}^{M \times N}$ such that $M \ll N$. The sparsity of the sensing matrix is kept low and it is classified as fixed row weight R matrix, where each row of $\mathbf{\Phi}$ contains exactly R non-zero entries. This allows sensing of maximum number of signal coefficients to obtain measurement vector **y**.

The main feature of the sensing matrix for Bayesian framework is that it can be represented as bipartite graph. We assume that a bipartite graph $\mathcal{G} = (\mathcal{U}, \mathcal{V}, \mathcal{E})$ represents the neighboring relations in $\mathbf{y} = \mathbf{\Phi x}$, such that $\mathcal{U} = \{1,2,3,\cdots,N\}$ represents the set of indices corresponding to each element in **x**, $\mathcal{V} = \{1,2,3,\cdots,M\}$ represents the set of indices corresponding to each element of measurement vector **y** and the set of edges connecting $\mathcal{U}$ and $\mathcal{V}$ can be defined as $\mathcal{E} = \{(j,i) \in (\mathcal{U} \times \mathcal{V}) | \varphi_{ji} = 1\}$, where φ_{ji} represents the jith element in $\mathbf{\Phi}$. The neighbor set of $\mathcal{U}$ will be $\mathcal{T}_{\mathcal{U}}(i) = \{j \in \mathcal{V} | (j,i) \in \mathcal{E}\}$ and the neighbor set of $\mathcal{V}$ will be $\mathcal{T}_{\mathcal{V}}(j) = \{i \in \mathcal{U} | (j,i) \in \mathcal{E}\}$.

4.3.2 Prior Model

In Bayesian framework, the selection of prior distribution plays a key role in the estimation of the sparsest solution out of infinite solutions for an under-determined system. Here we have considered two types of system models i.e.,

(1) Noiseless system model,

(2) Noisy system model.

In noiseless system model, the Rayleigh faded signal **x** is encoded without considering the noise factor i.e., $\mathbf{y} = \mathbf{\Phi x}$, while in noisy system model, AWGN also accounts for computation of measurement vector i.e., $\mathbf{y} = \mathbf{\Phi x} + \mathbf{n}$, where the additive noise vector

$\mathbf{n} = \mathbb{R}^{\boldsymbol{M}}$ is drawn from $i.i.d.$, zero-mean Gaussian noise distribution $\mathcal{N}(0, \sigma_n^2 \mathbf{I}_{\boldsymbol{M}})$, where σ_n^2 represents the variance of noise distribution and $\mathbf{I}_{\boldsymbol{M}}$ is identity matrix of order $M \times M$. We have shown that different features of each system model determine the need of a different prior model, for its optimal employment in BP for CS decoding algorithm.

4.3.2.1 Prior Model for Noiseless System Model

If **s** represents the state vector for **x** elements, then each signal coefficient $\mathrm{x_i}, i \in \mathcal{U}$ can be associated either with high state i.e., $s(i) = 1$, or it can be associated with low state i.e. $s(i) = 0$,where $s(i) \in \mathbf{s}$.

For Rayleigh faded signal **x**, the high state element is related to Rayleigh distribution as

$$f_{\mathbf{X}}(\mathbf{x}|\mathbf{s} = \mathbf{1}) = \left(\frac{\mathbf{x}}{\sigma_1^2}\right) \mathrm{e}^{-\frac{\mathbf{x^2}}{\mathbf{2\sigma_1^2}}} \tag{4.8}$$

where σ_1^2 represents the variance of Rayleigh distribution for signal coefficients associated with high state.

Similarly, the low state element in **x** can be related to a Spike distribution model as

$$f_{\mathbf{X}}(\mathbf{x}|\mathbf{s} = \mathbf{0}) = \delta(\mathbf{x}) \tag{4.9}$$

where $\delta(\mathbf{x})$ represents a Dirac distribution having a non-zero value in the range $\mathbf{x} \in (0-, 0+)$, such that $\int_{\mathbf{0}}^{\infty} \delta(\mathbf{x}) dx = 1$.

The Rayleigh-Spike prior density associated with noiseless system model is given by

$$f_{\mathbf{X}}(\mathbf{x}) = \mathrm{q}\left(\frac{\mathbf{x}}{\sigma_1^2}\right) \mathrm{e}^{-\frac{\mathbf{x^2}}{\mathbf{2\sigma_1^2}}} + (1 - \mathrm{q})\delta(\mathbf{x}) \tag{4.10}$$

Such type of priors have been used for strictly sparse signal models [47-50], since the prior easily characterizes the signals by σ_1 and q factors.

Since the elements in **x** are assumed to be $i.i.d.$ Rayleigh distributed, the prior density represents each ith signal coefficient independently.

4.3.3.2 Prior Model for Noisy System Model

For the noisy system model $\mathbf{y} = \mathbf{\Phi x} + \mathbf{n}$, the prior model should account for the Gaussian distribution associated with additive noise vector **n** along with Rayleigh and Dirac distribution.

For high state signal elements, when $i.i.d.$ Rayleigh distributed coefficient **x** adds up with $i.i.d.$ Gaussian noise coefficients **n**, then the resultant vector $\mathbf{z} = \mathbf{x} + \mathbf{n}$ would follow the probability distribution that is obtained after the convolution of probability distribution of **x** i.e.

$$f_{\mathbf{X}}(\mathbf{x}|\mathbf{s}=\mathbf{1}) = \left(\frac{\mathbf{x}}{\sigma_1^2}\right) e^{-\frac{\mathbf{x^2}}{\mathbf{2\sigma_1^2}}} \tag{4.11}$$

and the probability distribution of noise coefficient **n** i.e.,

$$f_{\mathbf{N}}(\mathbf{n}) = \left(\frac{1}{\sqrt{2\pi\sigma_{\mathrm{n}}^2}}\right) e^{-\frac{\mathbf{n^2}}{\mathbf{2\sigma_n^2}}} \tag{4.12}$$

The probability distribution for **z** is given by

$$f_{\mathbf{Z}}(\mathbf{z}|\mathbf{s}=\mathbf{1}) = \int_{\mathbf{0}}^{\infty} f_{\mathbf{X}}(\mathbf{x}) f_{\mathbf{X}}(\mathbf{z}-\mathbf{x}) dx \tag{4.13}$$

where $\mathbf{n} = \mathbf{z} - \mathbf{x}$,

$$f_{\mathbf{Z}}(\mathbf{z}|\mathbf{s}=\mathbf{1}) = \left(\frac{1}{\sqrt{2\pi}\sigma_n\sigma_1^2}\right)\int_{\mathbf{0}}^{\infty} \mathbf{x}e^{-\frac{\mathbf{x^2}}{\mathbf{2\sigma_1^2}}}e^{-\frac{(\mathbf{z}-\mathbf{x})^2}{\mathbf{2\sigma_n^2}}}\,dx \tag{4.14}$$

Evaluating this integral via integration by parts yields

$$f_{\mathbf{Z}}(\mathbf{z}|\mathbf{s}=\mathbf{1}) = \frac{\sigma_1\mathbf{z}}{(\sigma_1^2+\sigma_n^2)^{\frac{3}{2}}}\emptyset\left(\frac{\sigma_1}{\sigma_n}\frac{\mathbf{z}}{\sqrt{\sigma_1^2+\sigma_n^2}}\right)+\left(\frac{\sigma_n}{\sqrt{2\pi}\sigma_1^2+\sigma_n^2}\right)e^{-\frac{(\mathbf{z})^2}{\mathbf{2\sigma_n^2}}} \tag{4.15}$$

where $\emptyset\left(\frac{\sigma_1}{\sigma_n}\frac{\mathbf{z}}{\sqrt{\sigma_1^2+\sigma_n^2}}\right)$ is the cumulative distribution function (CDF) of standard normal random variable.

The low state signal coefficient in noisy system model is represented by Dirac distribution, as it is special form of the Gaussian density when $\sigma_0 \rightarrow 0$ [60]

The prior density for noisy system model would be

$$f_{\mathbf{X}}(\mathbf{x}) = \mathrm{q}\left(\frac{\sigma_1\mathbf{z}}{(\sigma_1^2+\sigma_n^2)^{\frac{3}{2}}}\emptyset\left(\frac{\sigma_1}{\sigma_n}\frac{\mathbf{z}}{\sqrt{\sigma_1^2+\sigma_n^2}}\right)+\left(\frac{\sigma_n}{\sqrt{2\pi}\sigma_1^2+\sigma_n^2}\right)e^{-\frac{(\mathbf{z})^2}{\mathbf{2\sigma_n^2}}}\right) \tag{4.16}$$
$$+(1-\mathrm{q})\delta(\mathbf{x})$$

In the following section, BCS approach to recover the signal has been discussed. The prior density models discussed in this section have been used to estimate the MAP distribution for the unknown signal elements for the noiseless and noisy measurement cases.

4.4 CS Decoding via BP

To recover the Rayleigh distributed signal **x** out of system models discussed above i.e. the noiseless system model and the noisy system model, we propose a Bayesian approach. The signal is recovered via BP as a MAP estimation problem. The sparsifying

prior density of **x** promotes the estimation of the sparsest solution that best matches with the linear projections **y** of sparse signal **x**. The signal recovery can be represented as

$$\hat{\mathbf{x}}_{MAP} = \arg\max f_{\mathbf{X}}(\mathbf{x}|\mathbf{Y} = \mathbf{y}) \tag{4.17}$$

where $\hat{\mathbf{x}}_{MAP}$ represents the recovered sparse signal **x** via MAP estimation

According to Bayesian theorem,

$$f_{\mathbf{X}}(\mathbf{x}|\mathbf{Y} = \mathbf{y}) = \frac{f_{\mathbf{Y}}(\mathbf{y}|\mathbf{X} = \mathbf{x}) f_{\mathbf{X}}(\mathbf{x})}{f_{\mathbf{Y}}(\mathbf{y})} \tag{4.18}$$

where $f_{\mathbf{X}}(\mathbf{x}|\mathbf{Y} = \mathbf{y})$ is the posterior distribution for **x**, $f_{\mathbf{Y}}(\mathbf{y}|\mathbf{X} = \mathbf{x})$ is the likelihood of the estimate and $f_{\mathbf{Y}}(\mathbf{y})$ is the marginal distribution. In Bayesian inference, marginal distribution plays no significant role in estimating posterior distribution. It only marginalizes the posterior distribution. Thus MAP estimation becomes

$$\hat{\mathbf{x}}_{MAP} = \arg\max f_{\mathbf{Y}}(\mathbf{y}|\mathbf{X} = \mathbf{x}) f_{\mathbf{X}}(\mathbf{x}) \tag{4.19}$$

It is obvious from above equation (4.15) that an accurate MAP estimation for **x** is possible when the sparsifying prior $f_{\mathbf{X}}(\mathbf{x})$ is selected according to the system model.

The BP provides the posterior density for MAP estimation in each iteration. The prior density initializes the BP process. Afterwards the posterior density of each signal element $\mathbf{x}_i$ is obtained and updated, while messages are being passed between the edges in factor graphs. Here sampled messages are considered to implement BP, where each message consists of the samples of the samples of the PDF [46]. Sampled message approach is adaptive in sense that various system models could be retrieved using it. When sampling step size is sufficient enough to store the PDF of the message under consideration, it also ensures faster convergence compared to parametric-message approach [57-59].

In CS decoding via BP we follow Bayesian rule, where the posterior density of each signal element $\mathbf{x_i}$ is represented in form of

$$posterior\ density\ =\ prior\ density \times \frac{likelihood}{evidence} \tag{4.20}$$

The marginal posterior density $f_{\mathbf{X}}(\mathbf{x}|\mathbf{Y}=\mathbf{y})$ is given by

$$f_{\mathbf{X}}(\mathbf{x}|\mathbf{Y}=\mathbf{y}) = f_{\mathbf{X}}(\mathbf{x}) \times \frac{f_{\mathbf{Y}}(\mathbf{y}|\mathbf{X_i}=\mathbf{x_i})}{f_{\mathbf{Y}}(\mathbf{y})} \tag{4.21}$$

where $f_{\mathbf{Y}}(\mathbf{y}|\mathbf{X_i}=\mathbf{x_i})$ is the likelihood, $f_{\mathbf{X}}(\mathbf{x})$ is the prior density for signal $\mathbf{x}$ and the evidence $f_{\mathbf{Y}}(\mathbf{y})$ only marginalizes the posterior density and does not enter into determining the relative properties. Since the measurements associated with $\mathbf{X_i}$ according to tree like property of $\mathbf{\Phi}$ i.e., $\{\mathbf{Y}_k : k \in \mathcal{T}_{\mathcal{U}}(i)\}$, are statistically independent given that $\mathbf{X_i}=\mathbf{x_i}$. The equation (4.17) can be re-written as

$$f_{\mathbf{X}}(\mathbf{x}|\mathbf{Y}=\mathbf{y}) \propto f_{\mathbf{X}}(\mathbf{x}) \times \sum_{j \in \mathcal{T}_{\mathcal{U}}(i)} f_{\mathbf{Y}_j}(\mathbf{y}|\mathbf{X_i}=\mathbf{x_i}) \tag{4.22}$$

Here each decomposition of likelihood $f_{\mathbf{Y}_j}(\mathbf{y}|\mathbf{X_i}=\mathbf{x_i})$ is the measurement density which is associated with the signal elements distributions and also the noise distribution for the noisy case. For noiseless case, the measurement density is given by

$$f_{\mathbf{Y}_j}(\mathbf{y}|\mathbf{X_i}=\mathbf{x_i}) = \delta_{\mathbf{Y}_j} \otimes \left(\bigotimes_{k \in \mathcal{T}_v(j) \setminus \{i\}} f_{\mathbf{X}_k}(\mathbf{x}) \right) \tag{4.23}$$

where $\delta_{\mathbf{Y}_j}$ is the probability density associated with each measurement vector element

$\mathbf{y}_j$ and $k \in \mathcal{T}_v(j) \setminus \{i\}\, f_{\mathbf{X}_k}(\mathbf{x})$ represents all the neighboring signal elements of $\mathbf{y}_j$ excluding $\mathbf{x}_i$. The $\otimes$ represents the operations of linear convolution, while $(\otimes f_{\mathbf{X}}(\mathbf{x}))$ represents the linear convolution of sequence of functions.

For the noisy case, the noise distribution $f_{\mathbf{N}_j}(\mathbf{n})$ also accounts for the measurement density i.e.

$$f_{\mathbf{Y}_j}(\mathbf{y}|\mathbf{X}_{\boldsymbol{i}} = \mathbf{x}_{\boldsymbol{i}}) = \delta_{\mathbf{Y}_j} \otimes f_{\mathbf{N}_j}(\mathbf{n}) \otimes \left(\bigotimes_{k \in \mathcal{T}_v(j)\setminus\{i\}} f_{\mathbf{X}_k}(\mathbf{x}) \right) \tag{4.24}$$

BP involves the process of exchanging and updating the probability density messages among the signal and the measurement coefficients, which relate to each other according to the edges in the bipartite graphs. It is mainly accomplished in two steps known as $multiplication$ and $convolution$. The marginal posterior for each $\mathbf{x}_{\boldsymbol{i}}$ is updated at every iteration.

The message passed from the ith signal coefficient to the jth measurement vector coefficient is called the $signal\ message$, and denoted as $\mathbf{m}_{i \to j}$, and similarly the message passed from the jth measurement vector coefficient to the ith signal coefficient is called the $measurement\ message$, denoted as $\mathbf{m}_{j \to i}$. The passing of the messages between the signal nodes and the measurement nodes can be well understood by Figure The signal message is the approximated density message of each signal element $\mathbf{x}_{\boldsymbol{i}}$, i.e. $\mathbf{m}_{i \to j} \approx f_{\mathbf{X}_i}(\mathbf{x}|\mathbf{y})$ and it is obtained from equation (4.22) by the multiplication of all the density messages associated with the neighboring measurement vector coefficients that are updated in previous iteration i.e.,

$$\mathbf{m}_{i\to j}^{l} = \eta\left[f_{\mathbf{X}}(\mathbf{x}) \times \prod_{k\in\mathcal{T}_U(i)\setminus\{j\}} \mathbf{m}_{k\to i}^{l-1}\right] \tag{4.25}$$

where $\mathbf{m}_{i\to j}^{l}$ denotes the signal message at lth iteration, $\eta[\cdot]$ is normalizing function such that $\int \mathbf{m}_{i\to j}^{l}\, d\mathrm{x} = 1$, and $\mathbf{m}_{k\to i}^{l-1}$ denotes the neighboring measurement message updated in previous iteration excluding that of $\mathbf{y}_j$.

4.1.

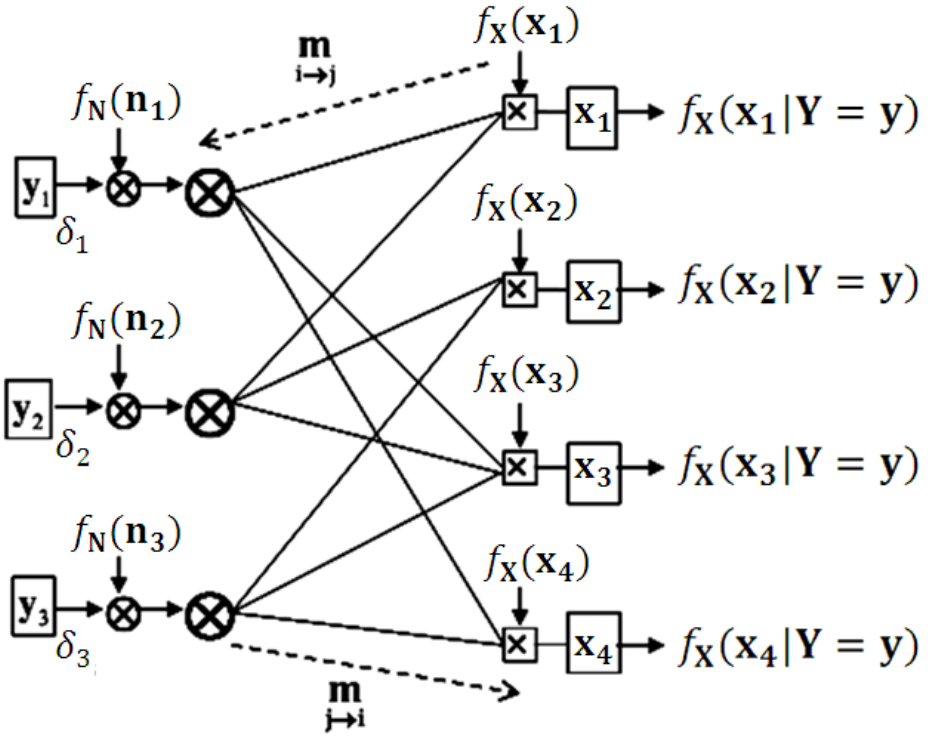

Figure: 4.1: Message passing between signal nodes and measurement nodes

In the same context, the measurement message is the approximated density message of each measurement vector coefficient $\mathbf{y}_j$, i.e. $\mathbf{m}_{j\to i} \approx f_{\mathbf{Y}_j}(\mathbf{y}|\mathbf{x})$. The measurement message is updated using equation (4.24), by the convolution of all the updated neighboring signal messages obtained i.e.,

$$\mathbf{m}_{j\to i}^{l} = \delta_{\mathbf{Y}_j} \otimes f_{\mathbf{N}_j}(\mathbf{n}) \otimes \left(\bigotimes_{k\in\mathcal{T}_v(j)\setminus\{i\}} \mathbf{m}_{k\to j}^{l} \right) \tag{4.26}$$

where $\mathbf{m}_{j\to i}^{l}$ is measurement message at lth iteration,and $\mathbf{m}_{k\to j}^{l}$ denote the neighboring signal messages updated excluding that of $\mathbf{x}_i$ in previous iteration.

For more efficient computation, the convolution operation in above equation (4.26) can be replaced multiplication operation via the use of Fast Fourier Transform (FFT), such that

$$\mathbf{m}_{j\to i}^{l} = \boldsymbol{\mathcal{F}}^{-1}\left[\boldsymbol{\mathcal{F}}\delta_{\mathbf{Y}_j} \times \boldsymbol{\mathcal{F}} f_{\mathbf{N}_j}(\mathbf{n}) \times \prod_{k\in\mathcal{T}_v(j)\setminus\{i\}} \boldsymbol{\mathcal{F}}\mathbf{m}_{k\to j}^{l} \right] \tag{4.27}$$

where $\boldsymbol{\mathcal{F}} \in \mathbb{C}^{D\times D}$is a Fourier matrix of size D. To evaluate the measurement density message efficiently via FFT, the sampling step for the sampled message in BP should be chosen appropriately such that number of samples is power of two.

In BP, while the signal and measurement messages are being exchanged and updated, the posterior density for each signal element $\mathbf{x}_i$ is being computed at every iteration as

$$f_{\mathbf{X}_i}^{l}(\mathbf{x}|\mathbf{y}) = \eta\left[f_{\mathbf{X}}(\mathbf{x}) \times \prod_{j\in\mathcal{T}_u(i)} \mathbf{m}_{j\to i}^{l} \right] \tag{4.28}$$

where $f_{\mathbf{X}_i}^{l}(\mathbf{x}|\mathbf{y})$ is the posterior density for $\mathbf{x}_i$ computed at lth iteration.

The maximum value of the density estimated for each signal element $\mathbf{x}_i$after T number of iterations determine the recovered value of each signal element i.e., $\hat{\mathbf{x}}_i$

4.5 Advantages over previous algorithms

The main advantage of the current algorithm over the previous algorithms suggested in literature is that it has been developed for practical channels like Rayleigh fading channels. Previously the CS algorithms were developed, considering AWGN channel where free space signal propagation takes place. Practically, the wideband signals undergo fading and their response to CS algorithms varies in Rayleigh fading channels compared to that in AWGN channels.

4.6 Summary

In this chapter, a BCS framework for Rayleigh faded channels is proposed, where a Rayleigh faded signal is recovered via BP. It is shown that decoding via BP is improved when the prior used in BP is according to the system model. The Rayleigh faded signal is recovered accurately, when Rayleigh-Spike prior is used for noiseless case. In noisy case, when AWGN noise is added to the system, prior is modified using convolution of Rayleigh-Gaussian-Spike model to improve the decoding process via BP. The MSE performance comparison for T number of iterations further assists that accuracy in the recovery of the Rayleigh faded signal is achieved when proper choice of prior is made.

Chapter 5

SIMULATIONS AND REULTS

5.1 Introduction

In this chapter, the performance of the CS algorithms for spectrum reconstruction and signal detection proposed in Chapter 3 and BCS algorithm for signal propagation in Rayleigh faded channels proposed in Chapter 4 has been evaluated via MATLAB simulations.

At first, the CS via basis pursuit approach proposed in Section 3.3 has been evaluated. A wide-band spectrum is reconstructed via CS using different number of linear combinations and different number of time samples. The estimated MSE gives an insight into the performance of the algorithm for different parameters.

In the next section the CS signal detection algorithm proposed in section 3.4 has been investigated and P_d and P_{fa} curves have been plotted for cognitive Bayesian energy detector.

In later section, the BCS algorithm for signal propagation in Rayleigh fading channels discussed in chapter 4, has also been investigated and compared with the performance of BCS algorithm for signal propagation in classic AWGN channel.

5.2 Wide-Band Spectrum Reconstruction via CS with Reduced Delay and Complexity

In this section, we evaluate the performance of the CS algorithm for wide-band spectrum reconstruction using basis pursuit approach, such that the sensing time aperture is

reduced along with the reduction in sampling rate. This approach consequently reduces the delay in spectrum sensing as well as complexity in wide-band spectrum sensing.

In this approach $S < N$ time samples of the wide-band spectrum are collected and the signal is reconstructed via CS using reduced number of linear combinations $M \ll N$. Thus, two parameters i.e., S and M affect the spectrum estimation via CS.

When the spectrum is reconstructed using reduced number of time samples S, it actually reduces the delay or latency caused in wide-band spectrum sensing. This makes the process more effective in terms of lesser chances of interference caused to primary transmission. Reduced number of linear combinations or measurements M, reduces the sampling rate; consequently the complexity of the spectrum sensing algorithm is reduced. We further evaluated the performance of the algorithm by estimating the MSE using equation $MSE = \left\| \mathbf{x}_f - \hat{\mathbf{x}}_f \right\|$.

We consider a wide-band spectrum with total bandwidth of $100\,MHz$. The Nyquist sampling rate for this wide-band signal is $200 \times 10^6 \frac{samples}{second}$. We assume that there are 10 channels in the wide-band spectrum each of $10\,MHz$, such that maximum 5 channels are active at a time to show the sparsity in the spectrum. We reconstruct the spectrum using different number of time samples S and linear combinations M. The numerical results of the reconstructed spectrum evaluated using l_1-minimization show that compression ratio must be at least $\frac{M}{N} = 45\%$, for 5 active channels. The compression ratio can be further reduced when the spectrum is more sparse i.e., 2 or 3 channels out of 10 channels are active.

In Figure 5.1, the frequency representation of the wide-band spectrum has been presented for $SNR = 10\ dB$ without compression. The spectrum shows 5 active channels out of 10 channels.

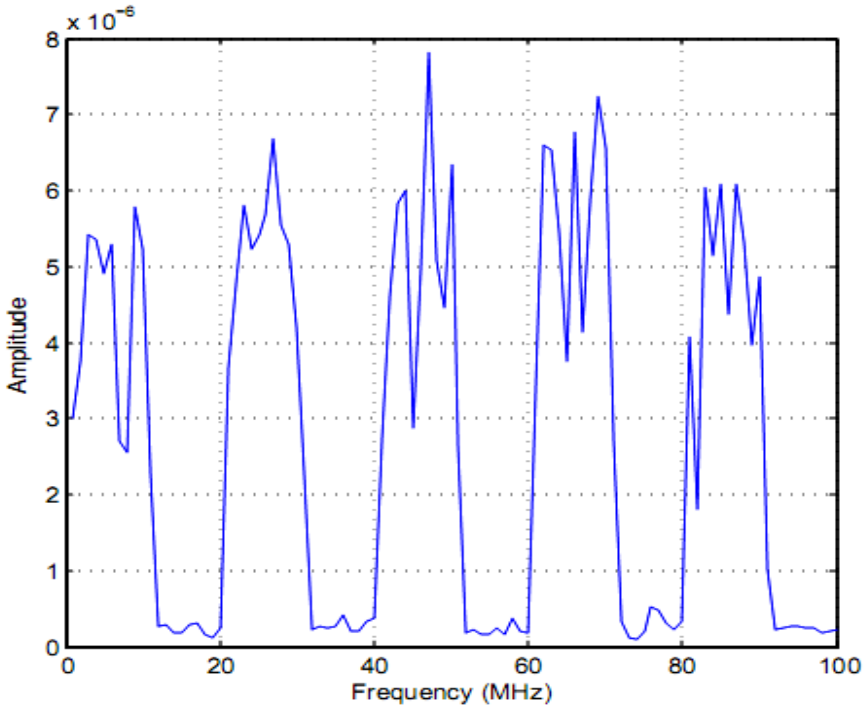

Figure: 5. 1: Wide-band spectrum, 5 out of 10 active channels, SNR = 10 dB

This spectrum is reconstructed via CS with compression ratio of $\frac{M}{N} = 50\%$, using $\frac{S}{N} = 50\%$ of time samples as shown in Figure 5.2. Though only half of the samples have been collected out of N total samples of the signal, but the figure shows that reconstructed frequency response of the signal is still a better approximation of the wide-band signal.

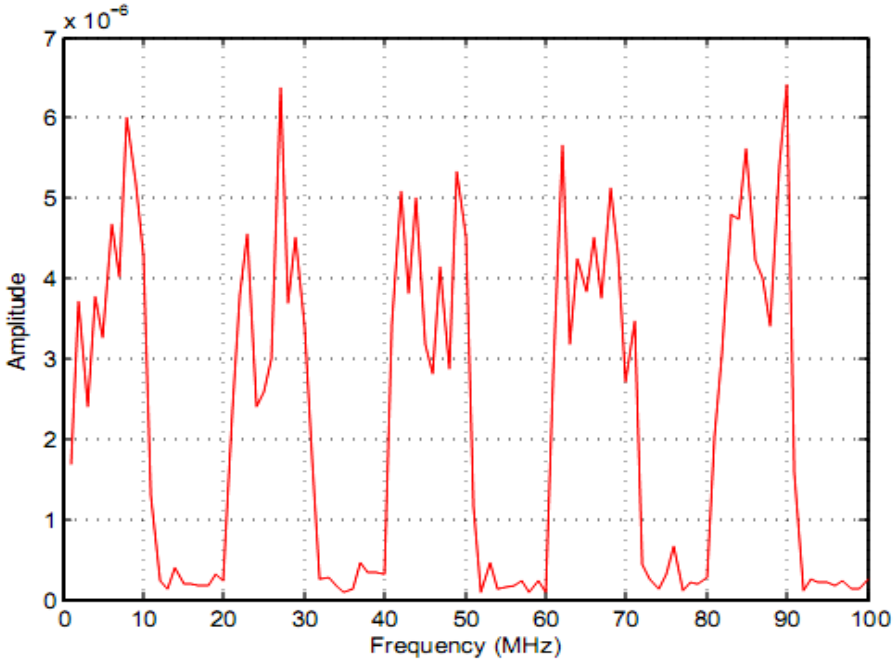

Figure: 5. 2: Reconstructed spectrum, M = N/2, S = N/2

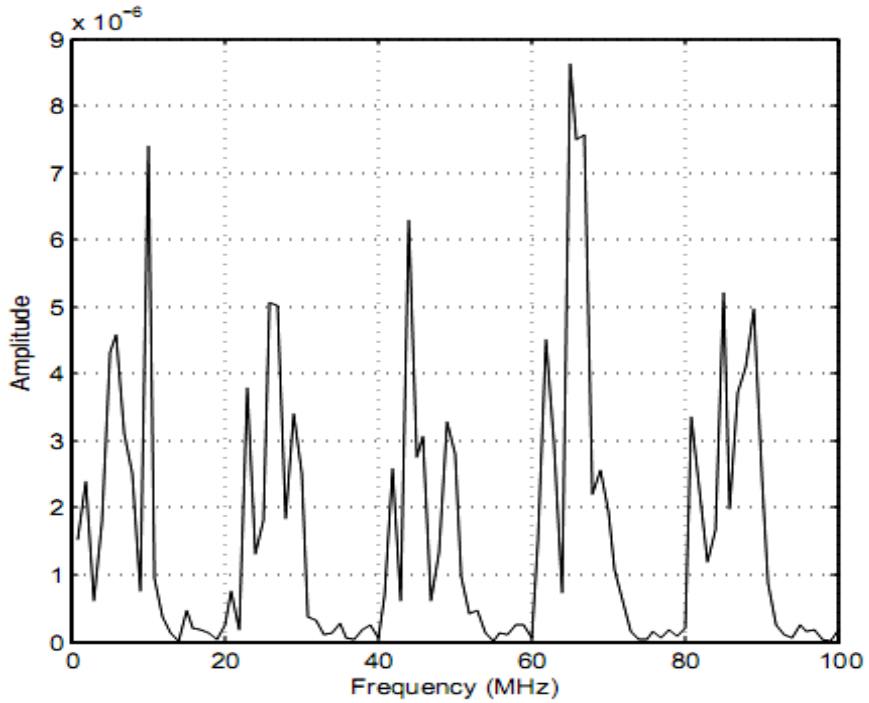

Figure: 5. 3: Reconstructed Spectrum, M = N/2, S = N/4

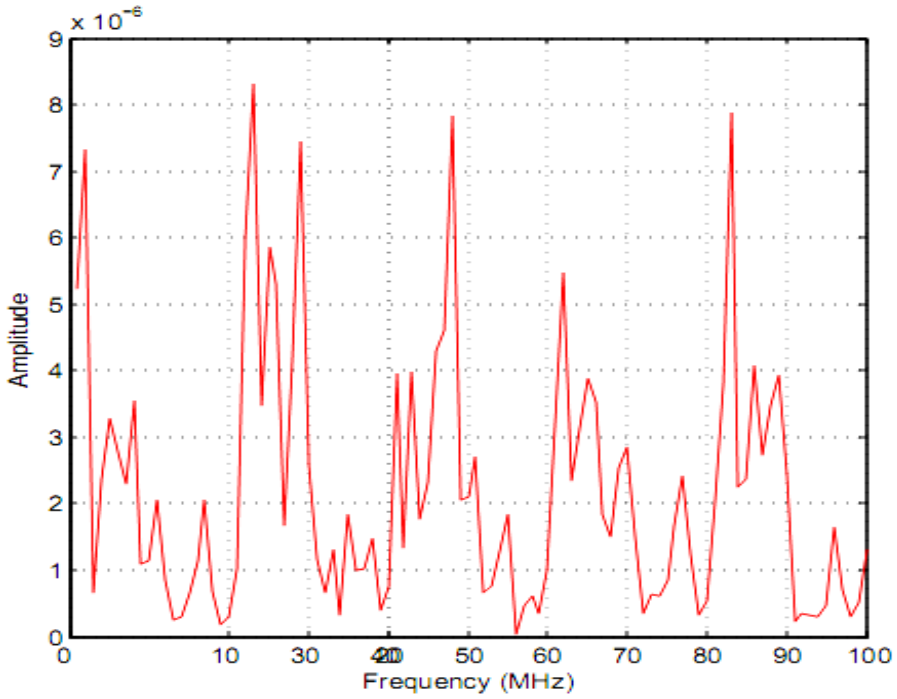

Figure: 5. 4: Reconstructed spectrum, M = N/2, sub-Nyquist sampling rate = 2/3

This scenario is of much importance in context of DSA using CR. A cognitive user only needs to detect the active primary transmission so that the secondary transmission causes no interference to it. As soon as the CR is able to reconstruct the spectrum using CS approach, it can identify the spectral holes and make the spectrum usage more effective.

This approach has been further investigated by reducing the number of samples up to $\frac{S}{N} = 25\%$. Still the reconstructed spectrum in Figure 5.3 shows that the active channels can be identified. Though the reconstructed spectrum is not as accurate as in previous case, but the energy accumulated in the channels is enough for energy detector to detect the active channels.

In section 3.3, we discussed that the complexity of the CS algorithm can be further reduced by distributing columns of zeros within the sensing matrix **Φ**. In this approach, the sampling is performed at a sub-Nyquist sampling rate. In Figure 5.4, the $100\ MHz$

wide-band spectrum has been reconstructed by taking samples at a sub-Nyquist sampling rate of 2/3, such that a zero column is inserted after every 2 columns of the sensing matrix. In this approach the reconstructed spectrum is again not a good approximation but energy detection can be performed on the spectrum to detect the occupancy pattern and identify the active channels in it.

In the following figures, MSE has been estimated for the spectrum reconstructed using different compression ratio M/N and sampling ratio S/N, to show the consistency of the results and compare the accuracy of the reconstructed spectrum.

Figure 5.5 shows that by reducing the number of samples taken out of the time signal, a better MSE performance can still be achieved. In the figure, we can see that when half of samples are taken i.e., the sampling ratio is $\frac{S}{N} = 50\%$, for compression ratio of $\frac{M}{N} = 50\%$, the performance of the algorithm improves compared to case when sampling ratio is $\frac{S}{N} = 100\%$, i.e., all time samples are taken. This can be justified by observing the lower limit of the number of measurements M required for spectrum reconstruction given by $M \geq cK \log(N/K)$.

When the number of time samples taken out of the wide-band signal is reduced such that $S < N$, then the signal length under consideration is reduced to S. The required number of measurements M can be further reduced according to the equation $M \geq cK \log(S/K)$. Thus the threshold for reconstruction is consequently reduced and the MSE performance of the algorithm is improved.

Same situation is observed when compression ratio is reduced up to $\frac{M}{N} = 25\%$, along with the reduction in signal length for up to $\frac{S}{N} = 25\%$. A better MSE performance is observed compared to the case of $\frac{M}{N} = 50\%, \frac{S}{N} = 25\%$.

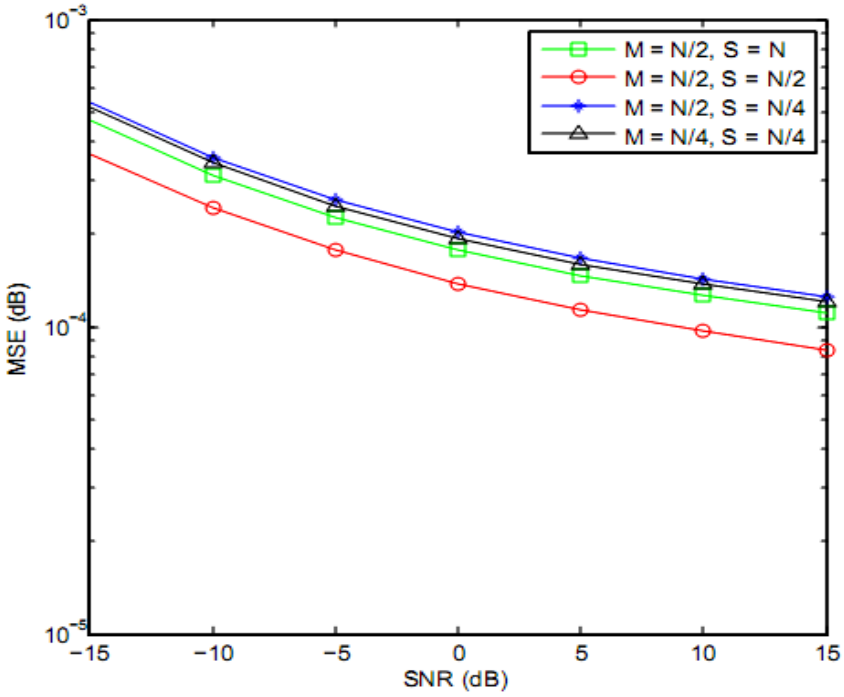

Figure: 5. 5: MSE estimated for reconstructed spectrum using different number of linear combinations and time samples

However in these two cases, the sampling ratio has been reduced beyond half, i.e., signal length is reduced much, which results in degradation in MSE performance compared to the case of $\frac{M}{N} = 50\%, \frac{S}{N} = 50\%$. This shows that we cannot reduce the sampling ratio beyond a certain limit. We require enough number of time samples of the signal for better reconstruction of the spectrum.

This concept of reducing the number of time samples of the signal can be efficient such that the decision about the spectrum occupancy pattern can be made faster as soon as the information about the reconstructed spectrum is available.

Another solution to reduce the sensing delay and complexity of the wide-band spectrum reconstruction using CS, is to distribute zero columns in the sensing matrix **Φ** i.e., compressive sampling is performed at a sub-Nyquist rate as discussed in section 3.3.

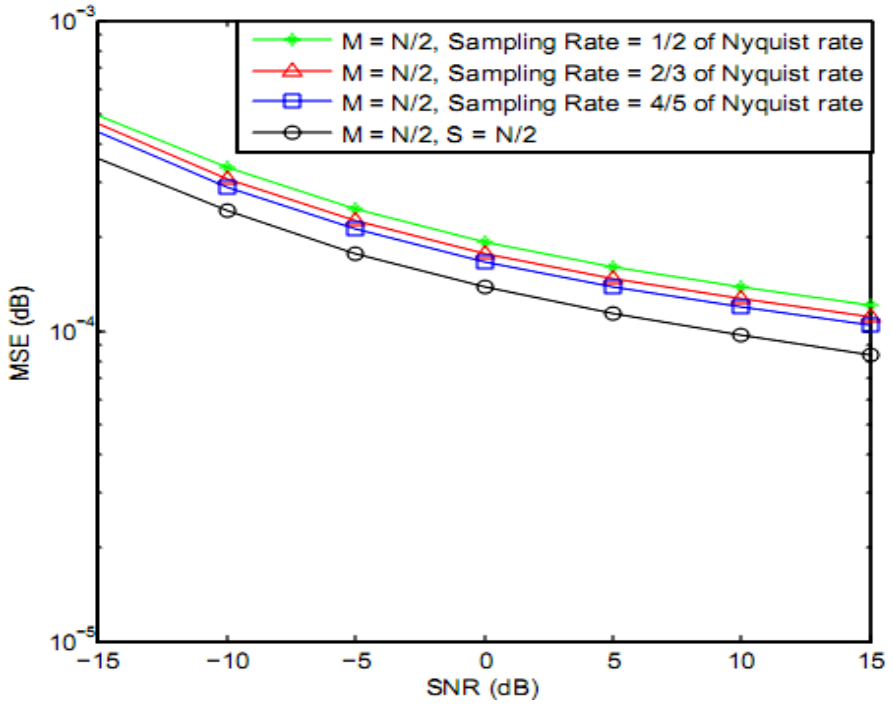

Figure: 5. 6: MSE estimated for reconstructed spectrum at sub-Nyquist sampling rates

The Figure 5.6 shows that a better MSE performance can be observed when the wide-band spectrum is reconstructed at a sub-Nyquist sampling rate by distributing columns of zeros within the compressive sensing matrix **Φ.** Though the MSE performance is not better compared to the previous cases where number of time samples S is reduced, but introducing zeros columns within the sensing matrix reduces the complexity of the CS algorithm.

To further emphasize on the results of a CS algorithm for wide-band spectrum reconstruction, we performed the algorithm by varying the number of active channels in the wide-band spectrum. Following figures show that when less number of channels is active in a wide-band spectrum, the spectrum is sparser, and the MSE performance of the CS algorithm improves.

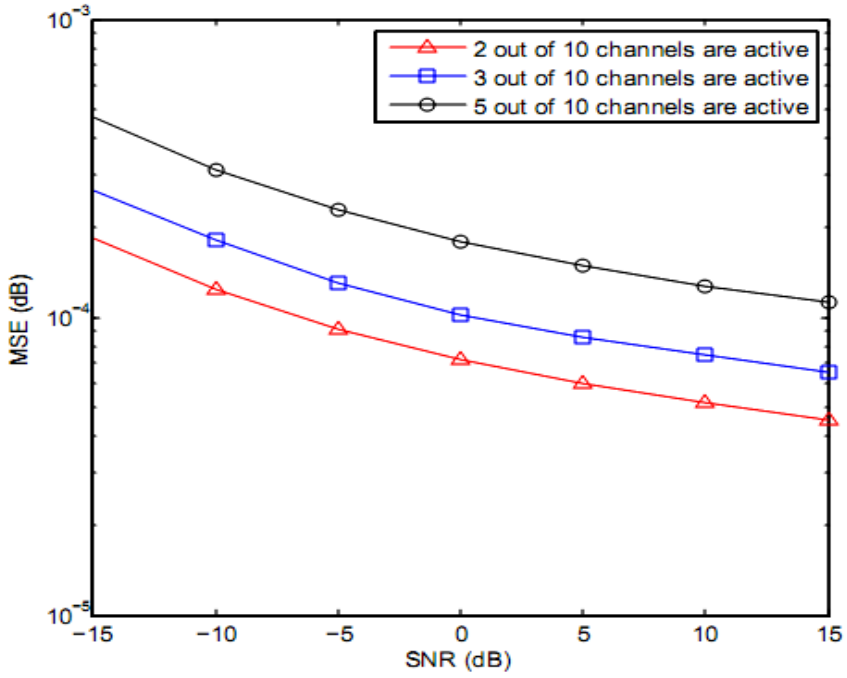

Figure: 5. 7: MSE performance of CS algorithm for wide-band spectrum reconstruction when number of active channels are varied to vary the sparsity level of the spectrum (M = N/2, S = N/2)

In Figure 5.7, the CS algorithm has been performed when reduced number of time samples is collected as discussed in section 3.3. It shows that the MSE performance of the algorithm improves when 2 out of 10 channels are active. In this case the sparsity level of the wide-band spectrum is higher compared to the cases in which 3 or 5 channels are active.

Similarly in Figure 5.8, the CS algorithm has been performed when columns of zeros are distributed in the sensing matrix **Φ**, to perform compressive sampling at a sub-Nyquist rate as discussed in section 3.3. It again shows consistency in results when MSE for 2 out of 10 active channels.

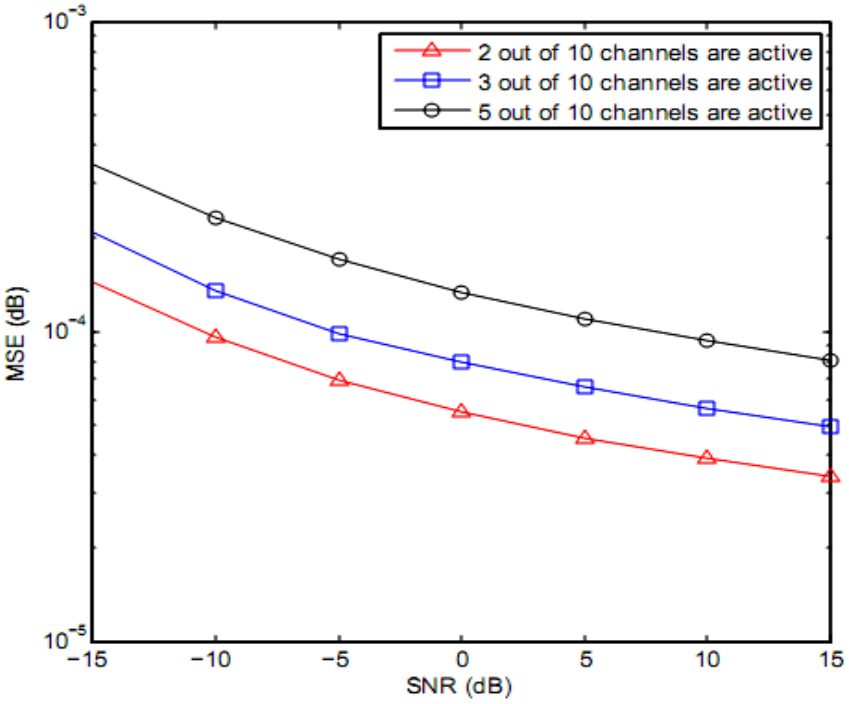

Figure: 5. 8: MSE performance of CS algorithm for wide-band spectrum reconstruction when number of active channels are varied to vary the sparsity level of the spectrum (M = N/2, Sampling rate = 2/3 of Nyquist rate)

5.2 Detection of Wide-band Signal via CS using CR Bayesian Energy Detector

In this section the performance of the CS algorithm for detection of wide-band signal has been investigated via MATLAB simulations. In section 3.4 a cognitive Bayesian energy detector has been proposed that estimates the energy occupied in each channel of the wide-band signal. The input wide-band signal is fed into M number of wide-band filters to estimate the energy in each channel, such that the energy vector **e** is reconstructed using CS via l_1-minimization approach.

As discussed in previous section, a wide-band signal is considered to be fed to CR Bayesian energy detector. It is assumed the wide-band signal is sparse such that there are 5 channels active at a time out of 20 channels in the wide-band. This wide-band signal is fed to different number of filters M, and the energy vector is estimated via CS. The estimated energy vector is compared with a threshold level to find the probability of detection P_d and probability of false alarm P_{fa} of the proposed algorithm.

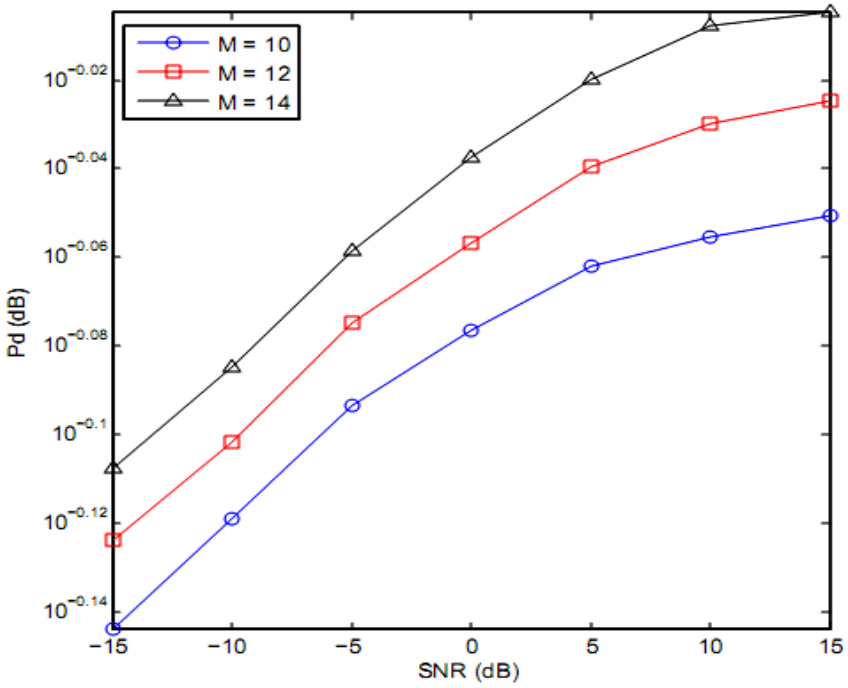

Figure: 5. 9: Probability of detection curve for detection of wide-band signal via CS

Figure 5.9 shows the probability of P_d curve obtained for the suggested algorithm and it shows that as the number of filters increases according to the number of channels in the wide-band spectrum, the P_d improves. For a wide-band spectrum containing 20 channels, at least there should be half of the number of filters in the CR energy detector for a better P_d.

Figure 5.10 shows the corresponding probability of false alarm P_{fa} for the wide-band signal detection algorithm.

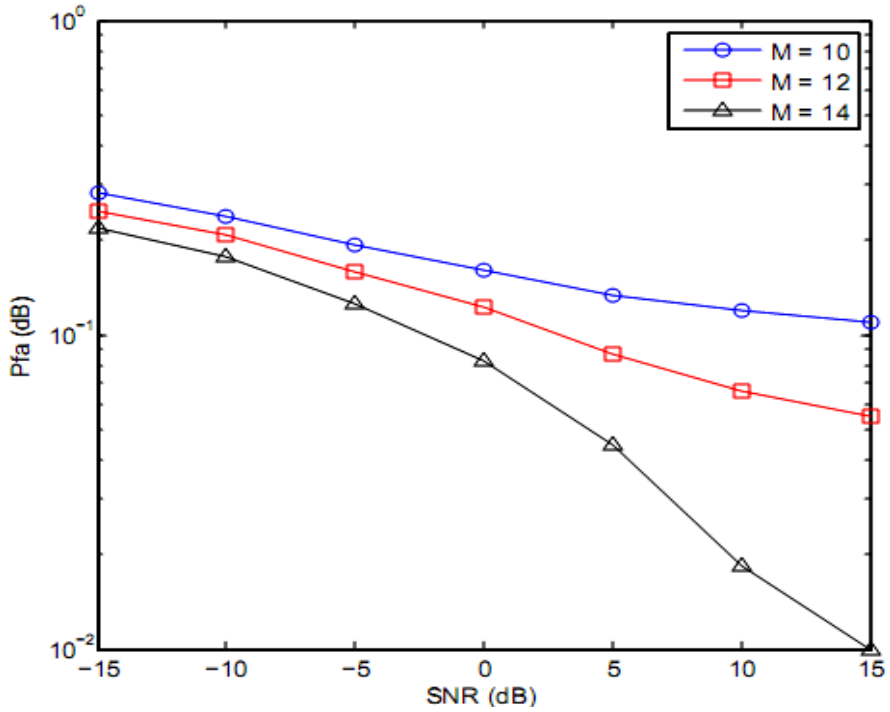

Figure: 5. 10: Probability of false alarm curve for detection of wide-band signal via CS

5.3 Bayesian Compressive Sensing Framework for Rayleigh Fading Channels

In this section, the performance of BCS algorithm, proposed in chapter 4, has been evaluated for Rayleigh fading channels using MATLAB simulation results. For a simple case, a wideband sparse signal **x** of length N is generated, such that the samples of the signal follow Rayleigh distribution. A compressive sensing matrix **Φ** is used to sense this sparse signal and M number of measurements is obtained for further recovery of the signal. To recover the Rayleigh faded signal via BP for noiseless case, we considered the Rayleigh-Spike prior given in equation (2.27). The sparse nature of the signal and the absence of noise results in almost accurate recovery of the signal.

However, in noisy case, when AWGN noise adds up in the measurement vector, the BCS recovery is not accurate using Rayleigh-Spike prior due to the noise distribution. The noise distribution affects the MAP estimation for BCS recovery of the Rayleigh faded signal.

To overcome this problem, the Rayleigh-Spike prior modified to match with the distribution of signal that is composed of Rayleigh coefficients and noise coefficients. The modified prior is composed of convolution of Rayleigh-Gaussian distribution for non-zero coefficients and Spike distribution for zero coefficients as shown in equation (4.16).

The BCS recovery of Rayleigh faded signal is performed for noisy case using the modified prior model and varied different parameters of the system model like sparsity level K, number of measurements M, number of samples in the prior distribution p etc., to see the performance of the algorithm.

According to the condition $M \geq c\,K\,\log(N/K)$ required for BCS approach, enough number of measurements is required for better BCS recovery of the signal. If the number of measurements is quite less, then the BCS recovery process does not perform well. In Figure 5.11, MSE has been plotted as a function of number of measurements M by varying row weight R for sensing matrix $\mathbf{\Phi}$.

When BP converges in $t = 5$ iterations and signal is recovered, MSE is calculated using the equation $MSE = \|\mathbf{\Phi}\hat{\mathbf{x}} - \mathbf{y}\|$, where $\hat{\mathbf{x}}$ is the reconstructed signal. MSE performance of the algorithm observed after $T = 10$ number of iterations using the modified prior, suggest that as M increases for signal length of $N = 1000$, the MSE error is reduced.

When row weight is small, i.e., $R = 10$, it misses some coefficients and results in poor recovery.

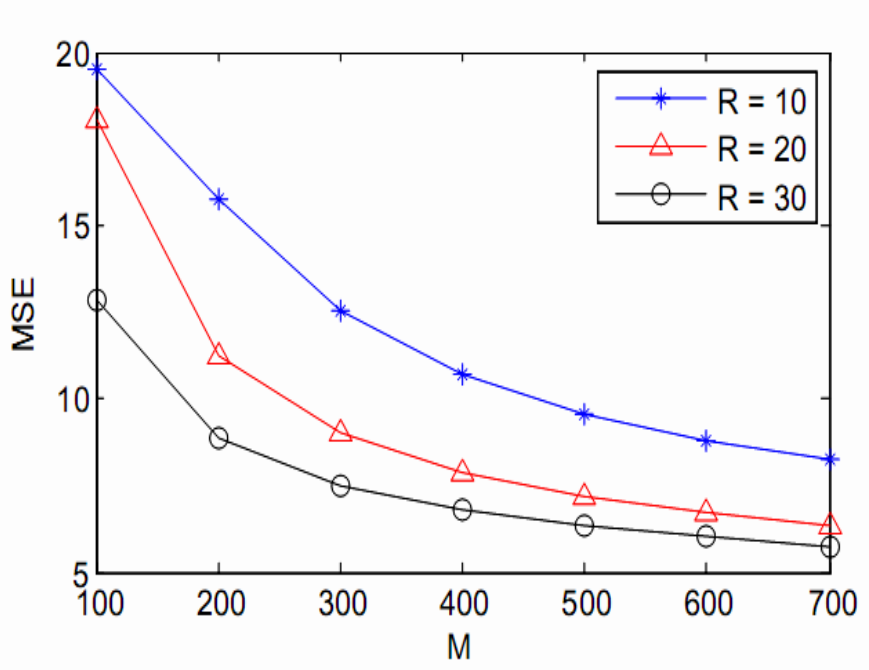

Figure: 5. 11: MSE as a function of M using different matrix row weights R for BCS recovery of Rayleigh faded signal using prior composed of convolution of Rayleigh-Gaussian distribution and Spike distribution, (N = 1000, K = 20, M = N/2)

MSE performance is improved when R is large and there are enough measurements M according to the signal length. MSE performance for $R = 30$ is better compared to that for R = 20, especially when $M \geq 400$ for $N = 1000$.

The above condition for enough number of measurements also shows that the length of signal N and the sparsity level K of the signal affect the performance of BCS recovery of the signal as well. In Figure 5.12, MSE has been plotted as a function of different values of K for a given N using the modified prior for BCS recovery of Rayleigh faded signal.

When the signal is more sparse, MSE is negligible. As the sparsity level K increases for given N, MSE becomes significant as shown in figure.

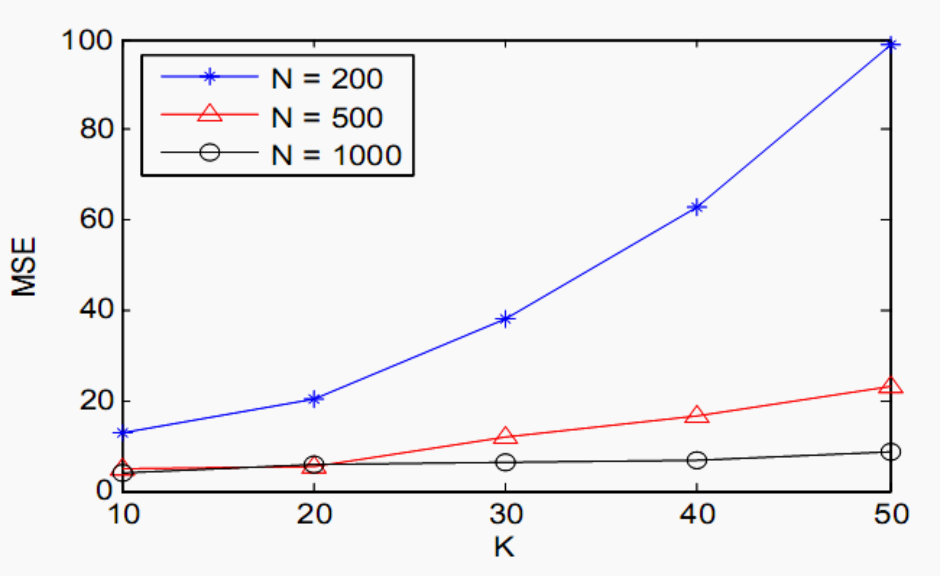

Figure: 5. 12: MSE as a function of sparsity level K for BCS recovery of sparse Rayleigh faded signal using prior composed of convolution of Rayleigh- Gaussian distribution and Spike distribution, (N = 200, 500, 1000, M = N/2)

For $N = 200$, MSE performance degrades when $K \geq 20$. Similarly for $N = 500$, MSE is significant when $K \geq 30$. However, for $N = 1000$ the algorithm performs better even for $K = 50$, which shows that performance of BCS algorithm improves when then the signal is more sparse.

As the sampled message approach has been used for the BCS recovery of Rayleigh faded signal, the sampling of the prior distribution also affects the outcome of BP. The convolution operation in BP to evaluate the density message, can be efficiently computed by using FFT as discussed in section 4.4. For efficient use of FFT, the sampling step should be chosen appropriately such that number of samples p is power of two.

In Figure 5.13, the MSE performance has been investigated for different number of samples of prior distribution. As the number of samples p increases, the MSE performance of the algorithm improves. When the number of measurements is lower, then the MSE performance of the algorithm is poor for all three cases.

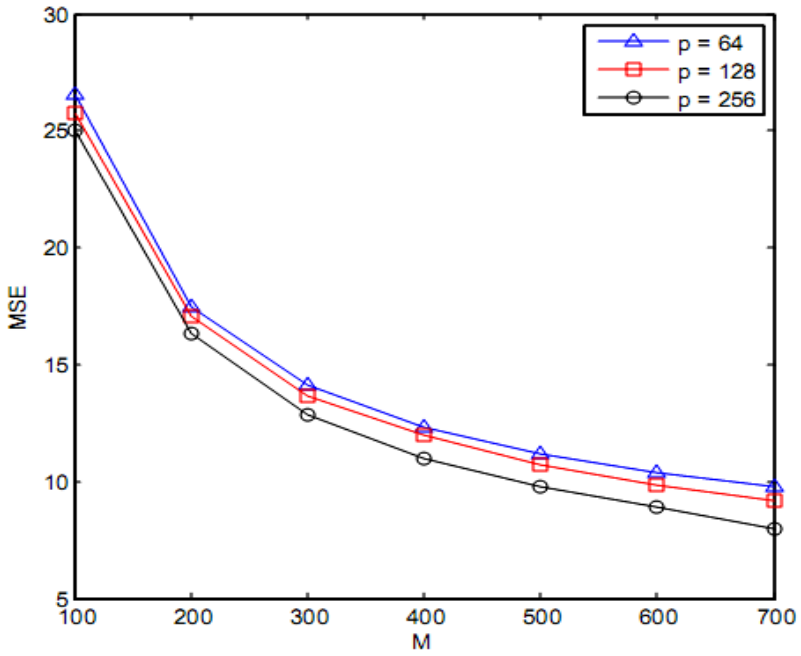

Figure: 5. 13: MSE as a function of number of measurements M using different number of samples for prior distribution p for BCS recovery of Rayleigh faded signal using prior composed of convolution of Rayleigh-Gaussian distribution and Spike distribution, (N =1000, K= 20, M = N/2)

The BCS recovery of the Rayleigh faded signal is performed for noisy case using different priors in Figure 5.14, and MSE is plotted as a function of different values of variance of noise σ_n^2.

The figure 5.14 shows that MSE is reduced, when decoding is performed for noisy system model using the modified prior that is composed of convolution of Rayleigh-Gaussian distribution for non-zero coefficients and Spike distribution for zero coefficients. However, when Gaussian prior is used for BCS recovery of the Rayleigh faded signal, MSE is significant.

When the level of noise that is added to the measurement vector increases, MSE further increases in case of Gaussian-Spike prior compared to the increase in MSE for modified prior composed of convolution of Rayleigh-Gaussian distribution and Spike distribution.

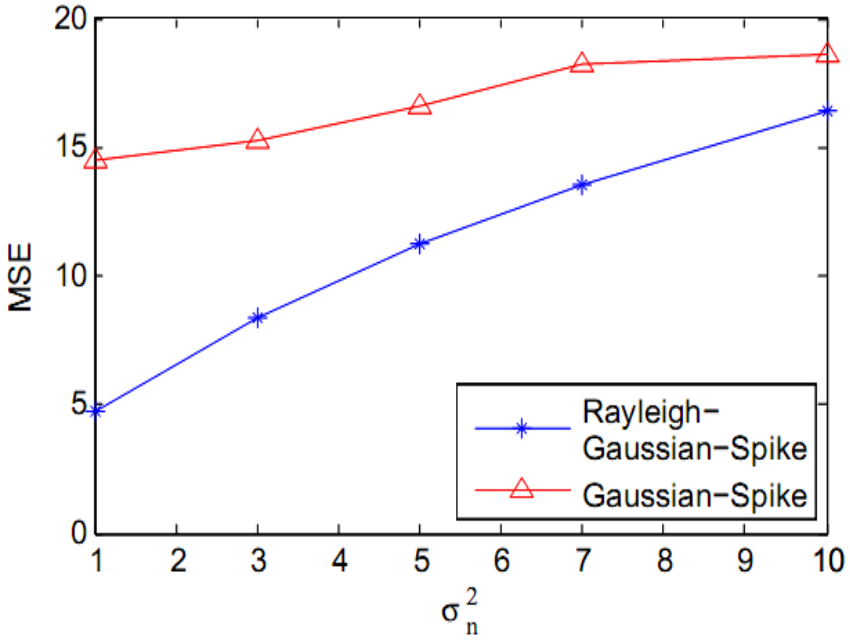

Figure: 5. 14: MSE as a function of noise variance $\boldsymbol{\sigma_n^2}$ where BCS recovery of sparse Rayleigh faded signal is done for noisy model using two types of priors, i.e., (1) Prior composed of convolution of Rayleigh-Gaussian distribution and Spike distribution (Rayleigh- Gaussian-Spike) (2) Gaussian-Spike prior (Gaussian-Spike) (N = 1000, K = 20, M = N/2)

This shows that appropriate prior should be used according to the signal model for BCS recovery process. The performance of the algorithm degrades, when properties of the prior are not according to the signal model.

To further emphasize on the appropriate choice of prior according to the system model, we varied the parameters for the system model and recovered the signal using the two above mentioned priors. In Figure 5.15, a sparse Rayleigh faded signal of length $N = 500$ is decoded using our modified prior composed of convolution of Rayleigh-Gaussian distribution and Spike distribution as well as the classical Gaussian-Spike prior.

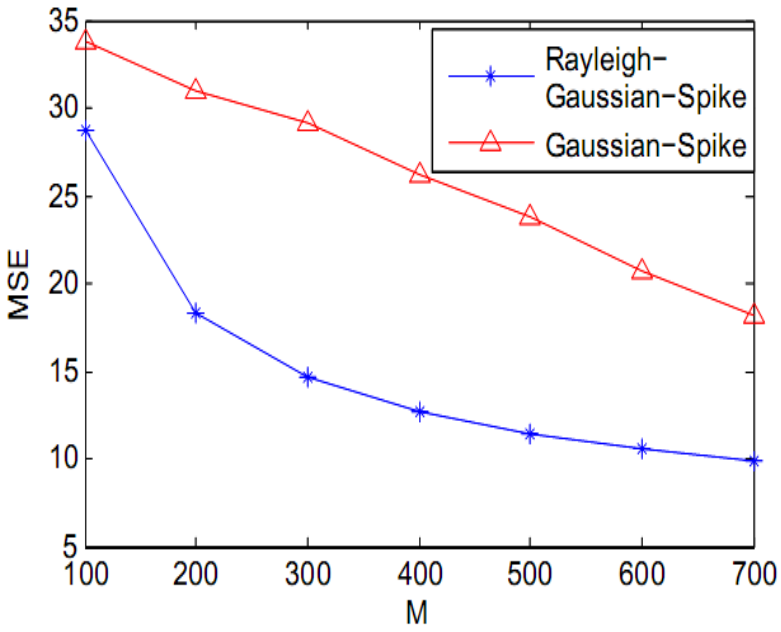

Figure: 5. 15: MSE as a function of number of measurements M where BCS recovery of sparse Rayleigh faded signal is done for noisy model using two types of priors, i.e., (1) Prior composed of convolution of Rayleigh-Gaussian distribution and Spike distribution (2) Gaussian-Spike prior

The MSE is plotted as function of number of measurements M, which shows that as M increases, MSE is reduced for our modified prior, while it is significant for Gaussian-Spike prior.

Similarly in Figure 5.16, MSE is plotted as function of sparsity level K for the two priors for a signal length of $N = 500$. It shows that when K increases; MSE is significant for Gaussian-Spike prior compared to our modified prior. These results show that when the prior model is in accordance with the system model, BP algorithm performs well, and MSE is reduced. The wide-band spectrum sensing via BCS can become more efficient when practical channels like Rayleigh fading channels are considered in the algorithm. The selection of the prior model according to the system model under consideration, improves the spectrum sensing process.

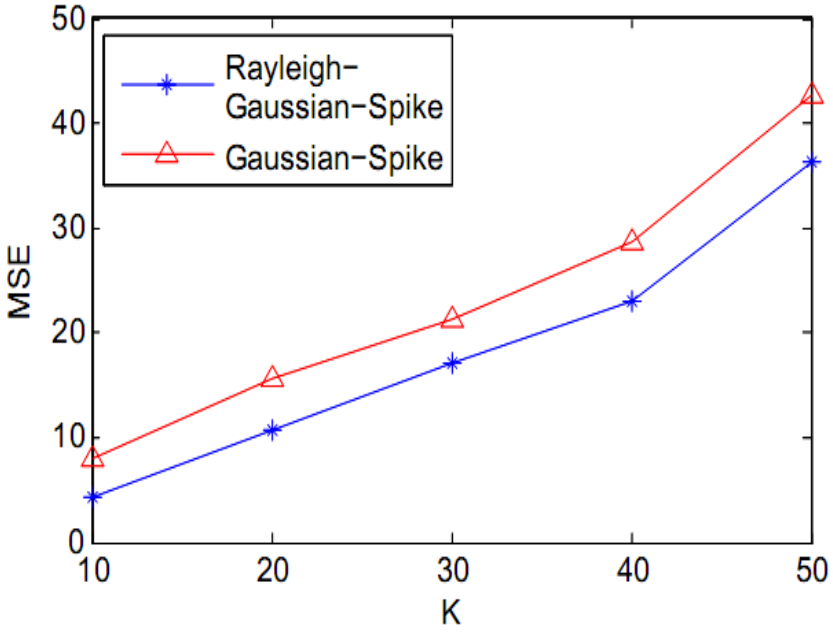

Figure: 5. 16: MSE as a function of sparsity level K where BCS recovery of sparse Rayleigh faded signal is done for noisy model using two types of priors, i.e., (1) Prior composed of convolution of Rayleigh-Gaussian distribution and Spike distribution, (2) Gaussian- Spike prior (N = 500, M = N/2, noise variance = 1)

Chapter 6

CONCLUSION AND FUTURE PERSPECTIVE

6.1 Conclusion

In this thesis, chapter 2 contains a detailed literature review of the field of CS and CR. Since DSA is one of the major application of CR, the major requirements and purpose of spectrum sensing is discussed. Different spectrum sensing techniques are discussed in terms of their hardware, performance and computational complexity. The issue of fading in wireless communication has also been highlighted which is not usually considered in spectrum sensing related literature. The basics of CS via basis pursuit approach as well as Bayesian inference approach, has been discussed. The prior distribution models conventionally used in BCS has been discussed in context of the requirement of appropriate model for the spectrum.

In chapter 3, solution to high data rates requirement for wide-band spectrum sensing has been proposed. A CS algorithm using basis pursuit approach can make wide-band spectrum sensing more efficient compared to conventional channel-by-channel scanning. The delay in detection of primary transmission can raise the risk of interference caused to the licensed users of the spectrum. This delay is reduced by reducing the size of the sensing matrix by using the feature of random coefficients selection of sensing matrix. Zero columns distributed in the sensing matrix consequently reduce the sensing time aperture as well as the complexity of the CS algorithm.

In chapter 4, the application of CS for spectrum sensing extends to a more practical scenario: i.e., where the signal of interest has undergone fading. By appropriately

modeling the prior distribution according to the fading distribution, an improvement in the MSE can be sought. Appropriate prior for Rayleigh faded sparse signal was derived and then used in the Bayesian Compressive Sensing framework. Simulation results show that the usage of appropriate prior distribution for faded sparse signal can result in an improvement in MSE.

6.2 Future Work

The CS algorithm suggested in chapter 3, to identify the occupied channels in the wide-band spectrum with reduced delay, can be further investigated to numerically analyze the threshold level up to which number of time samples can be reduced.

The BCS algorithm proposed in chapter 4, has been modified in terms of prior model selection for signal propagation in Rayleigh fading channels. This approach can be further extended to other practical channels like Rician fading channels, Dispersive fading channels etc.

Moreover, the determination of the sparsity level of the wide-band spectrum is another area which can be investigated to improve the efficiency of the CS algorithm.

In this study, the CR application for wide-band spectrum sensing and detection via CS has been considered. However this work can be applied to other applications as well.

BIBLIOGRAPHY

[1] F. Force, "Report of the spectrum efficiency working group," Federal Communications Commission, Technical Report, pp. 02–155, 2002

[2] J. Mitola III, "Cognitive radio for flexible multimedia communications," IEEE International Workshop on Mobile Multimedia Communications, 1999, (MoMuC '99), pp. 3–10, November 1999

[3] J. Mitola and G.Q. Maguire, "Cognitive radio: making software radios more personal," IEEE Personal Communications, vol. 6, pp.13-18, August 1999

[4] J. Mitola III, "Cognitive Radio: an integrated agent architecture for software defined radio," Royal Institute of Technology (KTH) Stockholm, Sweden, May 2000

[5] I. F. Akyildiz, W. Y. Lee and M. C. Varun, "NeXt generation/dynamic spectrum access/cognitive radio wireless networks: a survey," Computer Networks Journal, pp. 2127-2159, September 2006

[6] Y. Xing, R. Chandramouli, S. Mangold and S. Shankar, "Dynamic spectrum access to open spectrum wireless networks," IEEE Journal on Selected Areas in Communications, pp. 626-637, March 2006

[7] S. Haykin, "Cognitive radio: brain empowered wireless communication," IEEE Journal on Selected Areas in Communications, vol. 23, no 2, pp. 201-220, February 2005

[8] S. Shankar, C. Cordeiro, and K. Challapali, "Spectrum agile radios: utilization and sensing architectures," IEEE International Symposium on New Frontiers in

Dynamic Spectrum Access Networks (DySPAN) 2005, Baltimore, Maryland, USA, pp. 160-169, 8-11, November 2005

[9] H. Tang, "Some physical layer issues of wide-band cognitive radio systems," Proceedings of IEEE International Symposium on the New Frontiers in Dynamic Spectrum Access Networks (DySPAN) 2005, Baltimore, Maryland, USA, pp. 151-159, November 2005

[10] D. Cabric, S. M. Mishra and R. W. Brodersen, "Implementation issues in spectrum sensing for cognitive radios," in Proceedings of Asilomar Conference on Signals, Systems and Computers, Pacific Grove, California, USA, vol. 1, pp. 772-776, November 2004

[11] E. Candes, J. Romberg, and T. Tao, "Robust uncertainty principles: exact signal reconstruction from highly incomplete frequency information," IEEE Transaction on Information Theory, vol. 52, no. 2, pp. 489-509, February 2006

[12] D. Donoho, "Compressed sensing," IEEE Transaction on Information Theory, vol. 52, no. 4, pp. 1289-1306, April 2006

[13] E. Candes, M. Rudelson, T. Tao, and R. Vershynin, "Error correction via linear programming," IEEE Symposium on Foundations of Computer Science 2005, Pittsburgh, PA, pp. 668-681, October 2005

[14] E. J. Candes and M. B. Wakin, "An introduction to compressive sampling," IEEE Signal Processing Magazine, vol. 25, no. 2, pp. 21–30, March 2008

[15] S. Sarvotham, D. Baron and R. Baraniuk, "Compressed sensing reconstruction via belief propagation," Technical Report TREE0601, Rice University, Houston, TX, July 2006

[16] D. Baron, S. Sarvotham, and R. Baraniuk, "Bayesian compressive sensing via Belief propagation," IEEE Transaction on Signal Processing, vol. 58, no. 1, pp. 269-280, January 2010

[17] J. Neel, "Analysis and design of cognitive radio networks and distributed radio resource management algorithms," PhD Dissertation, EE Virginia Tech, September 2006

[18] K. Harrison, S. M. Mishra and A. Sahai, "How much white-space capacity is there?" Proceedings of IEEE International Symposium on the New Frontiers in Dynamic Spectrum Access Networks (DySPAN) 2010, Singapore, pp. 1-10, April 2010.

[19] FCC, "Unlicensed operations in the TV broadcast bands," Second Memorandum Opinion and Order, pp. 10-174, September 2010

[20] R. D. Hinman, "Application of cognitive radio technology to legacy military Waveforms in a JTRS (joint tactical radio system) radio," Military Communications Conference, MILCOM, pp 1-5, 2006

[21] M. McHenry, "NSF spectrum occupancy measurements project summary", Shared Spectrum Company, August 2005

[22] M. McHenry and D. McCloskey, "Spectrum occupancy measurements: Chicago, Illinois," Shared Spectrum Company, Technical Report, 2005

[23] "Use cases for cognitive applications in public safety communications systems: chemical plant explosion scenario," Public Safety Special Interest Group, Technical Report, February 2010

[24] M. M. Buddhikot, "Understanding dynamic spectrum access: models, taxonomy and challenges," Proceedings of IEEE International Symposium on New Frontiers in Dynamic Spectrum Access Networks (DySPAN) 2007, Dublin, pp. 649-663, April 2007

[25] Ofcom, "Simplifying spectrum trading: reforming the spectrum trading process and introducing spectrum leasing," Interim Statement Ofcom, April 2010

[26] C. Oestges and B. Clerckx, "MIMO wireless communications: from real-world propagation to space-time code design", Academic Press Elsevier, Oxford, UK, April 2007

[27] Q. Zhao and B. M. Sadler, "A survey of dynamic spectrum access," IEEE Signal Processing Magazine, vol. 24, no. 3, pp. 79-89, May 2007

[28] P. Marshall et al., "XG dynamic spectrum experiments, findings and plans Panel," Department of Defense DoD, Spectrum Summit, 2006

[29] A. Sahai, N. Hoven, and R. Tandra, "Some fundamental limits on cognitive radio," Proceedings of Allerton Conference of Communications, Control and Computing, pp. 131-136, October 2004

[30] B Saklar, "Digital communications: fundamentals and applications," Prentice Hall, Upper Saddle River, 2001

[31] D. Cabric, A. Tkachenko and R. W. Brodersen, "Spectrum sensing measurements of pilot, energy, and collaborative detection," IEEE Military Communications Conference (MILCOM) 2006, Washington, DC, pp. 1-7, October 2006

[32] D. Bhargavi and C. R. Murthy, "Performance comparison of energy, matched-filter and cyclo-stationary-based spectrum sensing," IEEE International Workshop

on Signal Processing Advances in Wireless Communications (SPAWC) 2010, pp. 1–5, June 2010

[33] R. Tandra and A. Sahai, "SNR walls for signal detection," IEEE Journal of Selected Topics in Signal Processing, vol. 2, no. 1, pp 4–17, February 2008

[34] A. Fehske, J. Gaeddert and J. H. Reed, "A new approach to signal classification using spectral correlation and neural networks," IEEE International Symposium on New Frontiers in Dynamic Spectrum Access Networks (DySPAN) 2005, Baltimore, USA, pp. 144–150, November 2005

[35] W Yue and B Zheng, "Spectrum sensing algorithms for primary detection based on reliability in cognitive radio systems," Computer Electrical Engineering Journal, vol. 36 no. 3, pp. 469–479, 2010

[36] V. Brik, E. Rozner, S. Banerjee and P. Bahl, "DSAP: a protocol for coordinated spectrum access," IEEE International Symposium on New Frontiers in Dynamic Spectrum Access Networks (DySPAN) 2005, Baltimore, USA, pp. 611-614, November 2005

[37] Z. Quan, S. Cui, A. H. Sayed, and H. V. Poor, "Optimal multiband joint detection for spectrum sensing in cognitive radio networks," IEEE Transactiuons on Signal Processing, vol. 57, no. 3, pp. 1128–1140, March 2009

[38] R. Lopez-Valcarce and G. Vazquez-Vilar, "Wideband spectrum sensing in cognitive radio: joint estimation of noise variance and multiple signal levels," IEEE 10^{th} Workshop on Signal Processing Advances in Wireless Communications (SPAWC) 2009, Perugia, pp. 96–100, June 2009

[39] Z. Tian and G. B. Giannakis, “Compressed sensing for wideband cognitive radios,” IEEE International Conference on Acoustics, Speech and Signal Processing (ICASSP) 2007, Honolulu, HI, vol. 4, pp. 1357–1360, April 2007

[40] V. Havary-Nassab, S. Hassan, and S. Valaee, “Compressive detection for wide-band spectrum sensing,” IEEE International Conference on Acoustics, Speech, and Signal Processing (ICASSP) 2010, Dallas, TX, pp. 3094-3097, March 2010

[41] J. C. Pesquet, H. Krim, and E. Hamman, “Bayesian approach to best basis selection,” IEEE International Conference on Acoustics, Speech, and Signal Processing (ICASSP), pp. 2634–2637, 1996

[42] F. Kschischang, B. Frey, and H. Loeliger, “Factor graphs and the sum-product algorithm,” IEEE Transaction on Information Theory, vol. 47, no. 2, pp. 498–519, February 2001

[43] H. Loeliger, “An introduction to factor graphs,” IEEE Signal Processing Magazine, vol. 21, no. 1, pp. 28–41, January 2004

[44] J. Yedidia, W. Freeman and Y. Weiss, “Understanding belief propagation and its generalizations,” Exploring Artificial Intelligence in the New Millennium, vol. 8, pp. 236–239, January 2003

[45] M. Pretti, “A message-passing algorithm with damping,” Journal of Statistical Mechanics: Theory and Experiment, issue 11, pp. 11008, 2005

[46] B. J. Frey and D. J. C. MacKay, “A revolution: belief propagation in graph with cycles,” Advances in Neural Information Processing Systems, vol. 10, pp. 479-485, 1998

[47] J. Kang, H. N. Lee and K. Kim, “On detection-directed estimation approach for noisy compressive sensing,” cs.IT, May 2012

[48] J. Kang, H. N. Lee and K. Kim, “Detection directed sparse estimation using bayesian hypothesis test and belief propagation”, cs.IT, November 2012

[49] J. Kang, H. N. Lee and K. Kim, “Bayesian hypothesis test for sparse support recovery using belief propagation”, cs.IT, February 2013

[50] H. Ishwaran and J. S. Rao, “Spike and slab variable selection: frequentist and bayesian strategies,” The Annals of Statistics, vol.33, pp.730-773, 2005

[51] L. He and L. Carin, “Exploiting structure in wavelet-based Bayesian compressive sensing,” IEEE Transaction on Signal Processing., vol. 57, no. 9, pp. 3488-3497, September 2009

[52] S. J. Sadiq, “Application of compressive sensing and belief propagation for channel occupancy detection in cognitive radio networks”, Master thesis, University of Toronto, 2011

[53] A. Ghasemi and E. S. Sousa, “Spectrum sensing in cognitive radio networks: requirements, challenges and design trade-offs,” IEEE Communications Magazine, vol. 46, no. 4, pp. 32–39, April 2008

[54] R. G. Gallager, “Low-Density Parity Check Codes,” MIT Press, Cambridge, MA, 1963

[55] X. Tan and J. Li, “Computationally efficient sparse Bayesian learning via belief propagation,” IEEE Transaction on Signal Processing, vol. 58, no. 4, pp. 2010-2021, April 2010

[56] M. Akcakaya, J. Park, and V. Tarokh, "A coding theory approach to noisy compressive sensing using low density frame," IEEE Transaction on Signal Processing, pp. 5369-5379, November 2011

[57] D. Guo and C. C. Wang, "Asymptotic mean-square optimality of belief propagation for sparse linear systems," Proceedings in IEEE Information Theory Workshop (ITW) 2006, pp. 194-198, October 2006

[58] M. J. Wainwright, T. Jaakkola and A. Willsky, "Tree-based re-parameterization framework for analysis of sum-product and related algorithms," IEEE Transaction on Information Theory, vol. 49, no. 5, pp. 1120-1146, May 2003

[59] S. Rangan, "Estimation with random linear mixing, belief propagation and compressed sensing," Proceedings in 44th Annual Conference Information Sciences and Systems (CISS) 2010, pp. 1-6, March 2010

[60] J. A. Tropp, "Just relax: convex programming methods for identifying sparse signals in noise," IEEE Transaction on Information Theory, vol. 52, no. 3, pp. 1030-1051, 2006